Renewable and Sustainable Energy Reviews 54 (2016) 1592–1610

Contents lists available at ScienceDirect

Renewable and Sustainable Energy Reviews

journal homepage: www.elsevier.com/locate/rser

Control techniques for three-phase four-leg voltage source inverters in autonomous microgrids: A review

Mohammad Reza Miveh [a,*], Mohd Fadli Rahmat [a], Ali Asghar Ghadimi [b], Mohd Wazir Mustafa [a]

[a] Faculty of Electrical Engineering, Universiti Teknologi Malaysia (UTM), 81310 Skudai, Johor, Malaysia
[b] Department of Electrical Engineering, Faculty of Engineering, Arak University, Arak, Iran

ARTICLE INFO

Article history:
Received 2 July 2014
Received in revised form
25 May 2015
Accepted 23 October 2015

Keywords:
Islanded microgrid
Microgrid control
Four-Leg voltage source inverter
Power quality

ABSTRACT

The application of the four-leg inverter as an effective interface for renewable and sustainable distributed energy resources (DERs) is gaining more attention with the advances in power electronics technology. One of the key technologies in inverter-based distributed generation (DG) systems is the four-leg voltage source inverter (VSI) that is utilized to operate in autonomous four-wire microgrids. Four-leg VSIs are becoming increasingly popular in four-wire microgrid, because they can not only achieve a proper control scheme in autonomous mode but also cope with the prescribed power quality requirements. The aim of this paper is to provide an overview of the main characteristics of recently used control strategies for four-leg VSIs operating in autonomous microgrids. First, two commonly-used four-wire inverter configurations are discussed, and their advantages and disadvantages are compared. Afterwards, the most up to date control techniques for three-phase four-leg VSIs operating in islanded microgrid from the reference frame point of view are described. Lastly, a comparative analysis is carried out where the benefits and drawbacks of each strategy are assessed, and then some suggestions are put forward for the future research.

Contents

1. Introduction

Gradual reduction of fossil fuels, poor energy efficiency and environmental pollution are three major problems the conventional power system faces today [1–3]. Furthermore, current

* Corresponding author. Tel.: +60 129730982; fax: +60 75557005.
E-mail address: mohammadreza.miveh@yahoo.com (M.R. Miveh).

http://dx.doi.org/10.1016/j.rser.2015.10.079
1364-0321/

Nomenclature

APF	Active Power Filters
DG	Distributed Generation
DVR	Dynamic Voltage Restorer
DER	Distributed Energy Resource
FCS-MPC	Finite Control Set Model Predictive Control
HPS	Hybrid Power System
ILC	Iterative Learning Control
PI	Proportional Integral
PR	Proportional Resonant
PID	Proportional Integral Derivative
PLL	Phase-locked loop
RER	Renewable Energy Resource
SHE	Selective Harmonic Elimination
SPWM	Sinusoidal Pulse Width Modulation
SCC	Symmetrical Components Calculator
SMC	Sliding Mode Control
SOGI	Second Order Generalized Integrator
STR	Self-tuner Regulator
3D SVPWM	Three-dimensional Space Vector Pulse Width Modulation
THD	Total Harmonic Distortion
VSI	Voltage Source Inverter
UPQC	Unified Power Quality Conditioner
UPS	Uninterruptible Power Supply
VUF	Voltage Unbalanced Factor

Fig. 1. Structure of a typical microgrid.

centralized power generation plants are facing the problem of the high cost of expansion, especially in developing countries [4]. Renewable Energy Resources (RERs) can address these problems; however, in order to successfully integrate such green generation technologies into distribution networks, a large number of technical and regulatory issues need to be addressed.

The use of RERs within microgrids is one of the promising approaches to cope with the aforementioned environmental and technical problems. A microgrid can be defined as a group of Distributed Generations (DGs), loads, power electronic devices and energy storage systems, which behaves as a controllable entity [5,6]. The structure of a typical microgrid is depicted in Fig. 1. It is capable of operating either in autonomous mode or in conjunction with the main grid [7]. Microgrids are being developed to enhance energy efficiency, improve power quality as well as the resilience of the power system, reduce transmission losses, decrease consumer prices, and successfully facilitate the utilization of RERs [8–10].

The four-leg inverter is widely utilized in four-wire microgrids to provide high-power quality supply for the consumers [11]. Typically, four-leg inverters are used to connect small power generation units in parallel with the grid or other sources [2]. They can not only feed power into the main grid, but also can perform as power quality conditioners at their grid-connected point such as Active Power Filters (APFs), Dynamic Voltage Restorers (DVRs) and Unified Power Quality Conditioners (UPQCs) [12–15]. On the other hand, it may be desirable for them to continue operating in autonomous mode as Voltage Source Inverters (VSIs) when voltages and frequency of the microgrid are no longer supported by the main grid [16]. Common examples of autonomous systems operating with four-leg VSIs include Uninterruptible Power Supplies (UPSs), single home, large communities, satellite stations, aircrafts and ship propulsion systems [11]. However, four-leg power electronic inverters must be controlled accurately in both grid-connected and autonomous modes so that their integration does not jeopardize the stability and performance of microgrids.

Despite their growing importance in microgrids, there exist several essential control problems associated with four-leg inverters in both grid-connected and autonomous modes. Autonomous and grid-connected modes of operation, power flow control, power quality control, neutral line provision, power sharing issues, anti-islanding and synchronization together comprise the key challenges associated with such inverters in microgrid applications [2,10,16]. Over the last decade, many original ideas are introduced and developed to address these challenges. Although the extensive number of review articles have been published on the control of single-phase grid-tie power converters [17–19], three-phase three-leg grid-connected power converters [15,18–21], three-phase four-leg grid-connected inverter [19] and three-phase three-leg VSIs in autonomous operation [2,5,10,22,23], there appears to be an absence of a comprehensive review on control strategies for three-phase four-leg VSIs in autonomous operation. Therefore, this paper is written with the aim of summarizing all the related works in this area and to present it as a single reference.

The main objective of this study is to provide a comprehensive review on recently used control strategies for three-phase four-leg VSIs in autonomous microgrid. Moreover, detailed explanation, comparison and discussion on such VSIs from the reference frame

point of view are achieved. Furthermore, some suggestions are put forward for the future research.The rest of this paper is organized as follows. In Section 2 two commonly used four-wire inverter configurations are discussed and their advantages and disadvantages are summarized. In Section 3 available control strategy from the perspective of the coordinate system for three-phase four-leg inverter is comprehensively reviewed. Comparative analysis of control structures and some suggestions for the future research are put forward in Section 4.

2. Neutral line provision in microgrids

The presence of a combination of single-phase and three-phase loads/DGs in microgrids has heightened the need for a neutral line to provide a current path for unbalanced loads [24]. In such microgrids, power electronic inverters should be supplied a mixture of unbalanced and nonlinear loads. Since most traditional six-switch inverters are designed for three-phase three-wire systems, their controllers are quite suitable for balanced three-phase loads [25]. The main challenges caused by unbalanced and nonlinear loads in microgrids, include the malfunctioning of protection devices and adjustable speed drives, losses in rotating machines as well as saturation of transformers [26–28]. Hence, inverters should be improved with a neutral connection. The provision of neutral connection in three-phase inverters provides the ability to control phase voltages independently [24]. In this section, two simple ways of providing a neutral connection for three-phase VSIs in three-phase four-wire systems are briefly introduced, and their advantages and disadvantages are critically discussed.

2.1. Split DC-link

The split DC-link topology is one of the more common ways of providing a neutral point for three-phase VSIs in three-phase four-wire systems [29]. This configuration can be provided using two capacitors. Indeed, the DC-bus is split into a pair of capacitors, and the neutral path connects to the midpoint of the capacitors [30].

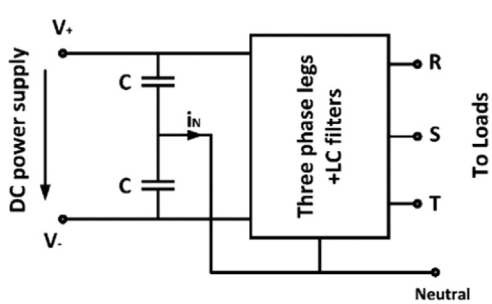

Fig. 2. Three-phase inverter with split DC-link capacitors.

The configuration of the split DC-link is shown in Fig. 2. Since the neutral current of APFs only includes AC component, and their fundamental components are quite small, the split DC-link topology can work well in these applications [30]. The implementation of this topology in three-level inverters is relatively simple. Moreover, it needs fewer semiconductors in comparison with other topologies [31]. However, it needs an expensive and a large capacitor to achieve equal voltage sharing between the split capacitors [32]. Another weakness with this configuration is that under severe unbalanced and nonlinear conditions, a large neutral current flows through the neutral path and cause a perturbation in the control scheme.

2.2. Four-leg inverter

Recently, researchers have shown an increasing interest in using the three-phase four-leg inverters because of their capability to effectively handle the unbalanced loads in four-wire systems [33,34]. In this topology, the neutral point is provided by connecting the neutral path to the midpoint of the additional fourth leg, as shown in Fig. 3. Although this configuration does not need to utilize large and expensive capacitors and provides lower ripple on the DC-link voltage, the use of two extra switches leads to a complicated control scheme [24]. Moreover, the AC voltage in this configuration can be about %15 higher, in comparison with the split DC-link [32]. An analytical comparison between these two topologies is presented in Table 1. It is generally concluded that the split DC-link is not appropriate for inverters, which supply power to possibly unbalanced loads in three-phase four-wire systems. On the other hand, the four-leg inverters have the significant potential to handle unbalanced and nonlinear conditions.

3. Available control techniques for four-leg VSIs in autonomous microgrids

It may be desirable for power electronic inverters to continue operating in autonomous mode when voltages and frequency of the microgrid are no longer supported by the main grid. In this circumstance, the voltage and frequency of the microgrid should be controlled using Distributed Energy Resources (DERs). Since islanding operation requires the implementation of appropriate load sharing mechanisms to balance sudden active power mismatches, it is significantly more challenging than the grid-connected mode [35]. Furthermore, the physical inertia of islanding operation is quite smaller than the grid-connected mode [36]. More importantly, for an autonomous microgrid with a large number of nonlinear or imbalanced loads, introducing a suitable compensation method to obtain accurate reactive, imbalance, and harmonic power sharing is very important. Hence, the islanding mode of operation requires an adequate control and management

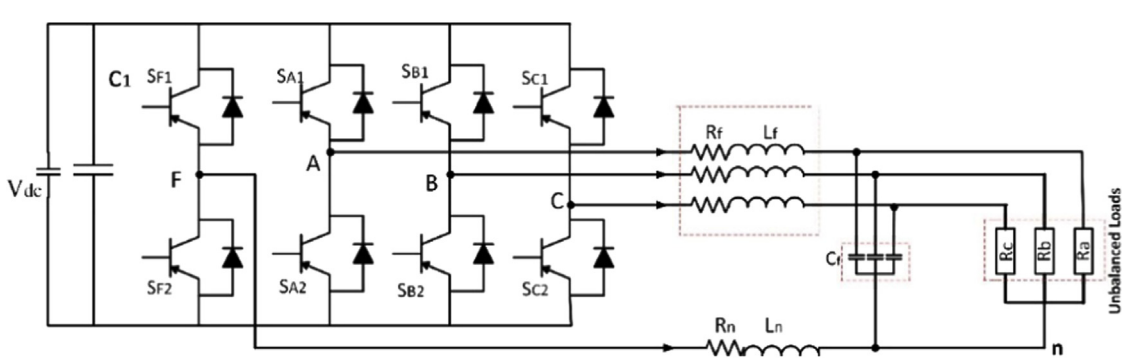

Fig. 3. Topology of four-leg inverter.

Table 1
Performance comparison of split DC-link and four-leg inverters.

Split DC-link topology		Four-leg topology	
Advantages	Disadvantages	Advantages	Disadvantages
Simple topology. The need for fewer semiconductor. Simple current tracking control.	Unequal voltage sharing between split capacitors. The need for expensive capacitors. Severe unbalanced and nonlinear loads cause a perturbation in the split voltages. The need for neutral point balancing strategy.	The ability to handle unbalanced and nonlinear conditions. Low DC-bus voltage. The output AC voltage can be about %15 higher than the output of split DC-link topology. Lower ripple on the DC-link voltage.	The need for two extra switches. Complicated control strategy.

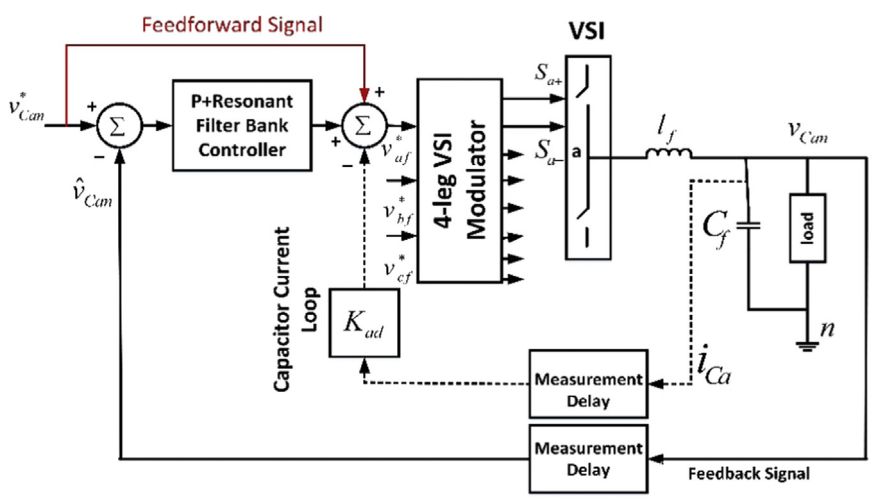

Fig. 4. Block diagram of the control system presented by Demirkutlu et al.

systems to satisfy the power quality requirements for sensitive load.

For autonomous microgrids, the power quality should be maintained in much the same way as with Hybrid Power Systems (HPSs) and UPSs [37–39]. According to the IEEE standards [37,38], the Voltage Unbalanced Factor (VUF) and the Total Harmonic Distortion (THD) should be maintained below 2% and 5% for sensitive loads, respectively. Voltage and frequency control, active and reactive power sharing control, power quality control and optimizing the microgrid operating cost together comprise the key principles of microgrid control structure in islanding mode [10,16].

Even though the control of DC to three-phase three-leg inverter in autonomous mode has been extensively assessed in recent years, the control of DC to four-leg inverter has received relatively little attention. To date, various strategies in different reference frames have been introduced and developed to control the four-leg VSI in stand-alone mode. These techniques from the reference frame point of view are precisely illustrated and critically discussed in the following subsections.

3.1. Natural abc frame control structure

The abc frame is one of the most widely used structures for the control of electronic power inverters [20]. It has been extensively utilized for nonlinear controllers such as the hysteresis control [21]. Meanwhile, linear controllers such as the Proportional Integral (PI) and Proportional Resonant (PR) are also commonly used in the abc frame control structure [18]. In this part, the most up to date control techniques for four-leg VSI in the abc frame are precisely presented.

3.1.1. Available control techniques for four-leg VSI in the natural abc frame

In [40], the authors present a scalar control approach to regulate the output voltages of a three-phase four-leg inverter operating in a stand-alone four-wire power supply. In this scheme, each phase of the four-leg inverter is controlled independently in the abc reference frame [41]. As shown in Fig. 4, the suggested method in each phase comprises a resonant-filter bank in combination with a Proportional (P) controller, a capacitor current feedback loop and a feedforward voltage loop. The main reason behind using the resonant-filter bank is to obtain a very high gain at a desired resonant frequency and zero gain elsewhere. The resonant-filter bank consists of a fundamental-frequency resonant-filter controller and a set of harmonic frequency resonant-filter controllers, as depicted in Fig. 5. It can effectively mitigate the impact of nonlinear and unbalanced loads. Additionally, to improve the output voltage dynamic response the P controller is added to the resonant-filter bank.

Despite its benefits, one of the main limitations with this resonant-filter-bank is that it cannot provide an accurate dynamic response under step load changes. To cope with this challenge, the capacitor current feedback loop (with a K_{ad} gain) is added to the control scheme. It has the ability to provide active damping and enhance the load disturbance rejection characteristic. Furthermore, a command voltage feedforward loop is added to the filter for the purpose of accurate command tracking. The proposed controller can be provided a proper output-voltage regulation and low harmonic distortion under unbalanced and nonlinear load conditions.

The hysteresis voltage regulator is one of the most well-known approaches to control the output voltages of power inverters in

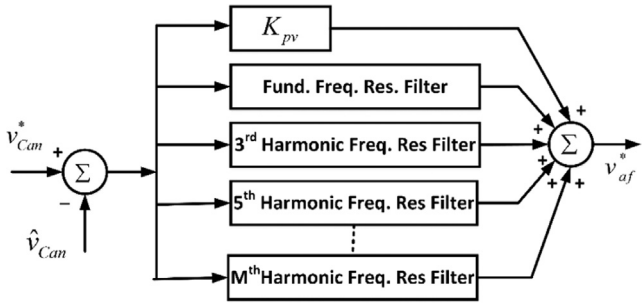

Fig. 5. Per-phase P+resonant-filter-bank controller structure proposed by Demirkutlu et al.

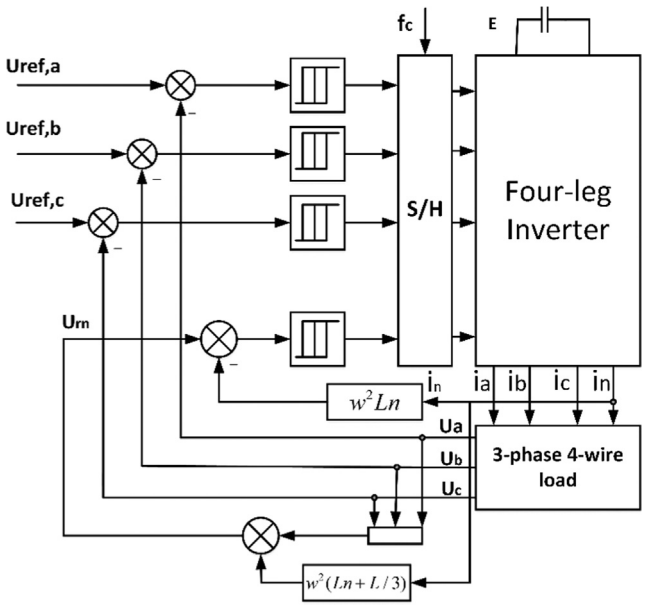

Fig. 6. Conventional hysteresis control structure for a three-phase four-leg inverter.

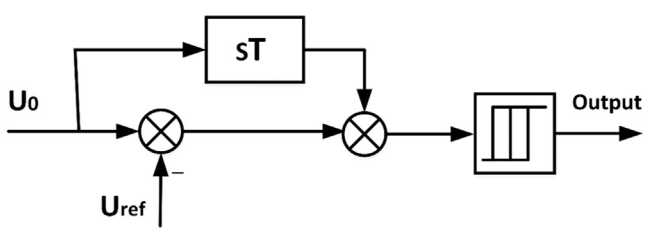

Fig. 7. Voltage hysteresis control with differential module proposed in [44].

RERs. It operates based on the nonlinear controller loop with hysteresis compensators [42]. The main target of these compensators is to design an adaptive band to obtain a fixed switching frequency [43]. The conventional voltage hysteresis control employed for a four-leg inverter is depicted in Fig. 6 [44]. This strategy uses the instantaneous voltage value to measure the differences between the feedback voltage and the reference value; afterwards, this difference is sent to the hysteresis compensator. Based on this difference and the width of the hysteresis loop the state of switches can be changed. This method is easier to implement than carrier-based approaches [42]. Nevertheless, it is characterized by the limitation of a non-constant switching frequency, irregular switching and slow dynamic response [17]. An improved hysteresis control strategy based on a differential negative feedback module is proposed in [44] to address these challenges. In this study, a differential negative feedback loop is

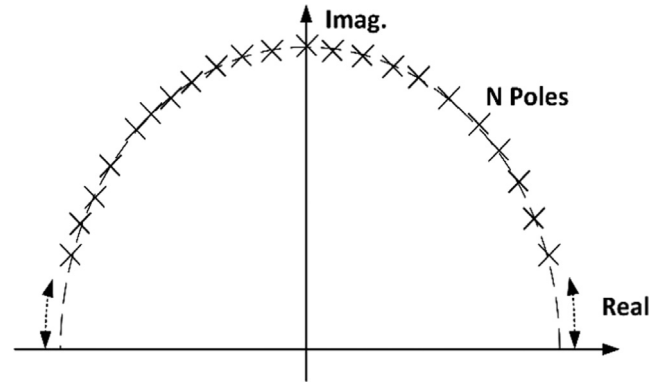

Fig. 8. Poles of (3) on the unit circle in the z-plane.

designed to improve the overall performance of the conventional hysteresis controller. The structure of the differential negative feedback loop is illustrated in Fig. 7. Considering u_0 as the feedback voltage, u_{ref} the reference value and the hysteresis width equal to $2h$ in Fig. 6, the following equation can be expressed for the conventional hysteresis control:

$$u_0 \simeq u_{ref} \pm h \tag{1}$$

The use of the differential module causes the difference between $u_0 + T\frac{du_0}{dt}$ and u_{ref} is sent to the compensator, and the actual hysteresis width h_1 becomes $h_1 = h - T\frac{du_0}{dt}$. In this structure, if the $\frac{du_0}{dt}$ is small, h_1 is big, otherwise if the $\frac{du_0}{dt}$ is big, h_1 is small. Therefore, the u_0 can immediately track the u_{ref}. The use of this structure leads to accurate tracking of the feedback signal by the reference signal.

A straightforward way to control a four-leg inverter with periodic disturbances is to use the repetitive feedback controller. It has been derived from the idea of Iterative Learning Control (ILC) [45]. This simple learning control has the capability to eliminate the periodic disturbances using the concept of the internal model principle [46]. Indeed, it is an alternative to a parallel combination of an integral regulator, several resonant controllers and a simple P compensator. Commonly, a low-pass filter is used in combination with the repetitive controller to reduce the high-frequency resonant peaks of the controller gain [47]. The work by Cárdenas et al. [48], presents a repetitive control technique to achieve low load-voltage THD in a four-leg matrix converter feeding non-linear loads. This controller produces N roots on the unit circle in the z-plane using the following equation:

$$Z^N - 1 = 0 \Rightarrow \text{Angle}(Z^N) = 0 \tag{2}$$

The transfer function of the repetitive controller can be presented as:

$$G_c(Z) = \frac{k_{cz}}{1 - Z^{-N}} \tag{3}$$

where k_{cz} is the controller gains in different frequencies. As depicted in Fig. 8, it provides N resonant poles on the unit circle in the z-plane, thereby eliminating the periodic distortions caused by nonlinear loads. However, the key problem with N poles located on the unit circle is that they reduce the phase margin of the system below a satisfactory value [47]. Hence, some extra compensators need to be incorporated within the repetitive controller to enhance the phase margin of the control loop. The structure of the proposed repetitive controller is shown in Fig. 9. The implementations of the repetitive controller and lead compensator are done based on the design procedure reported in [49]. The topology reported in [49] is chosen because it provides a simple implementation. In this paper, the repetitive controller is added to the conventional controller $C(z)$ proposed in [49]. In Fig. 9, $Q(z)$

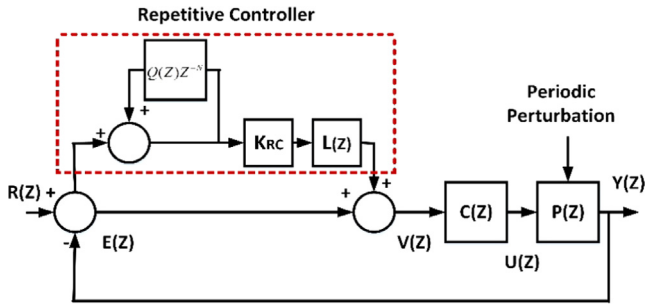

Fig. 9. Repetitive control structure presented by Cárdenas et al.

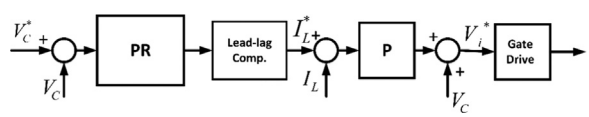

Fig. 10. Control block diagram proposed in [50].

corresponds to a low-pass filter with the following transfer function:

$$Q(z)=\frac{y_p\left(z^{-p}+z^{P}\right)+y_{p-1}\left(z^{-(p-1)}+z^{P-1}\right)+\ldots+y_0}{2y_p+2y_{p-1}+\ldots+y_0}. \tag{4}$$

where $y_0>y_1>\ldots>y_p$. It is used to improve the stability of the system and reduce the high-frequency gain of the proposed controller. $P(z)$ corresponds to the plant connected to the four-leg inverter, which can be different based on the type of load. $U(z)$ is the demanded voltage, which is the input to the Three-dimensional Space Vector Modulation (3D SVM) algorithm. K_{rc} is the gain of the repetitive controller. A lag network ($L(z)$) is also used to reduce the high-frequency gain of the suggested controller.

In [50], a droop-based control strategy is offered to control the parallel operation of two four-leg VSIs in an autonomous microgrid. The main objective is to share unbalanced and nonlinear loads between two DGs such that proper sinusoidal output voltages provide for the loads. The block diagram of the control loops in each phase is shown in Fig. 10. The proposed method comprises an internal current loop, an external voltage controller and a lead–lag compensator in the abc coordinate system. The inner current loop is implemented by a simple P controller, whereas the voltage loop is realized using the PR regulators in the abc reference frame. The lead–lag compensator is used to improve the stability of the system. To effectively share the unbalanced and nonlinear loads between four-leg inverters a droop control scheme in the abc frame is also adopted based on the design procedure reported in [51]. It is implemented using the positive sequence active and reactive powers. Additionally, a virtual output impedance loop is used to improve the performance of the droop controller. The suggested method has the ability to independently control the phase voltage of four-leg VSIs.

The Finite Control Set Model Predictive Control (FCS-MPC) has been used in many studies for control of electric power converters [52–54]. The basic idea of this approach is to minimize the forecast error so that the reference voltage can be tracked accurately without any error [11]. Similar to the carrier-less modulation schemes, this method operates with the variable switching frequency. To date, various predictive voltage control strategies have been introduced to control the output voltages of power inverters [31,54–56]. A predictive load voltage control for a two-level three-leg VSI is analyzed in [31], by considering symmetrical loads. This approach has been developed for a four-leg inverter with the same load model in [56]. The key problem with this study is that it has modeled based on the three-wire system that reported in [31]. Hence, it is important to modify the model of the system for the four-wire systems.

An improved FCS-MPC strategy with an output *LC* filter for a four-leg VSI is presented in [57]. In this approach, the behavior of the voltages for 16 possible switching states using the novel discrete-time model is predicted; afterwards, it is evaluated using a cost function. The switching state that minimizes the cost function is selected and applied at the next sampling instant. Additionally, the reliability of neutral-leg semiconductor switches has been also enhanced by reducing their switching frequency. The block diagram of the suggested control scheme is presented in Fig. 11. For the sake of simplicity, one-step prediction is used in this study. The control strategy requires the computation of the 16 possible conditions in sampling instant (k), which would minimize a given cost function in the ($k+1$) sampling instant. The switching state that gives minimal value for the cost function is chosen and applied by the system during all of the ($k+1$) period. The cost function is defined as follows:

$$g(k+1)=[v_o^*(k+1)-v_o(k+1)]^2+\lambda_{swc}\left|S_n(k+1)-S_{n,opt}(k)\right| \tag{5}$$

where λ_{swc}, $v_o^*(k+1)$ and $v_o(k+1)$ are the weighting factor, the extrapolated reference and the predicted load voltage, respectively. Moreover, $S_n(k+1)$ is the predicted neutral-leg switching signal, and $S_{n,opt}(k)$ is the optimal gating signal in the previous sample (k). The first term is related to the reference tracking of load voltages, while the second term is used to attenuate the neutral-leg switching frequency. The generation of references completely depends on the application of the power converter in the four-wire system. As the proposed strategy is implemented for islanding operation, the references are on the basis of the load appliance rating. This control strategy is developed using two-sample-ahead prediction horizon in [58] to obtain high-performance operation for the four-leg inverter. The performance of the one-sample-ahead and two-sample-ahead prediction horizon is also compared to evaluate their capabilities in terms of reference tracking error and THD. According to this study, the suggested two-sample-ahead prediction horizon is more appropriate for high-power applications where lower switching frequency operation is required.

Sliding Mode Control (SMC) is becoming increasingly popular in power electronic applications due to its superior performance

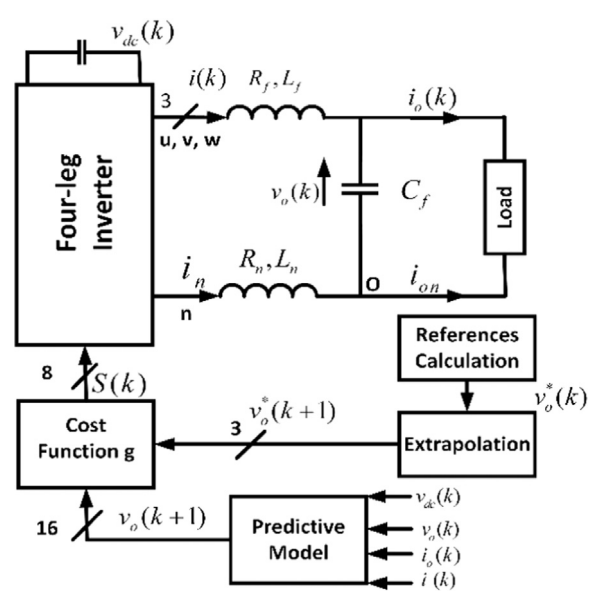

Fig. 11. Block diagram of the controller proposed in [57].

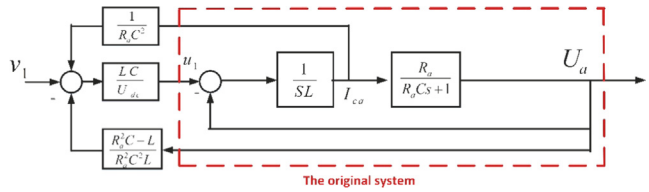

Fig. 12. Diagram of the inverter system based on the state feedback.

characteristics such as good operation against parameter variations and a high stability over a wide range of operating conditions [59,60]. This nonlinear controller consists of a switching term that can take the form of on-off control. A serious weakness with this controller, however, is that it suffers from the chattering problem [60]. In [61], by combining SMC with state-feedback control, an improved control scheme is designed to optimize controller design and enhance static and dynamic performances of a three-phase four-leg inverter. For the sake of simplicity, the linear coordinate change matrix and the state variable feedback equations are obtained using diffeomorphism relationship. The original complex system is represented into three independent simplified systems using the mathematical model. The equivalent block diagram of the inverter for the A-phase based on the state feedback is presented in Fig. 12. Sliding surfaces and quasi-sliding mode compensators are then employed to control the output voltages that track references. Based on the system relative degrees (r), these controllers are designed for the linear systems.

First, the SMC approach for the A-phase is designed, and then is expanded for the B-phase and C-phase based on the symmetry of the three-phase system. The state variable feedback equations for the A-phase are obtained as:

$$\dot{z_1} = \frac{\partial h_1(X)}{\partial X}\dot{X} = \frac{x_1}{R_a C} - \frac{x_4}{C} = z_2. \tag{6}$$

$$\dot{z_2} = \frac{\partial (L_f h_1(X))}{\partial X}\dot{X} = \left(\frac{1}{LC} - \frac{1}{R_a^2 C^2}\right)x_1 + \frac{x_4}{R_a C^2} - \frac{U_{dc}}{LC}u_1 = v_1. \tag{7}$$

where $X = [x_1 x_2 x_3 x_4 x_5 x_6]^T = [u_a u_b u_c i_{ca} i_{cb} i_{cc}]^T$ is state variable, including the output voltages and inductor currents and $Y = [h_1(X) h_2(X) h_3(X)]^T$ is voltage error as output variables. $L_f h = (\partial h/\partial X) f$ is also defined as the Lie derivative of f and h.

The sliding surfaces for A-phase can be explained as:

$$\sigma_1 = \frac{d(z_1 - z_1^*)}{dt} + \lambda_1 \frac{d(z_1 - z_1^*)}{dt} + \lambda_0 \int d(z_1 - z_1^*)dt = z_2 + \lambda_1 z_1 + \lambda_0 \int z_1 dt \tag{8}$$

where $\lambda_0, \ldots, \lambda_{r-1}$ are coefficients and should be chosen so that the tracking error dynamics become stable. The quasi-sliding mode is selected based on the boundary layer approach law. Δ is the boundary layer thickness, and this approach law can be defined as:

$$v_{1n} = -\varepsilon . sat(\sigma_1/\Delta) \tag{9}$$

The three-phase sliding mode controllers are explained as:

$$V = \begin{bmatrix} v_1 \\ v_2 \\ v_3 \end{bmatrix} = \begin{bmatrix} v_{1eq} + v_{1n} \\ v_{2eq} + v_{2n} \\ v_{3eq} + v_{3n} \end{bmatrix} = \begin{bmatrix} -\lambda_1 z_2 - -\lambda_0 z_1 - \varepsilon . sat(\sigma_1/\Delta) \\ -\lambda_1 z_4 - -\lambda_0 z_3 - \varepsilon . sat(\sigma_2/\Delta) \\ -\lambda_1 z_6 - -\lambda_0 z_5 - \varepsilon . sat(\sigma_3/\Delta) \end{bmatrix}. \tag{10}$$

where v_{1eq} is the continuous control input in A-phase that forces $\dot{\sigma}_{1,} = 0$.

The proposed SMC is analyzed for $|\sigma| \le \Delta$ and $|\sigma| > \Delta$. For the former case, the closed-loop transfer function of the system is a third order linear system. Consequently, the parameters of the controller can be designed based on the linear theory. For linear control system, the parameters of controller is chosen according to

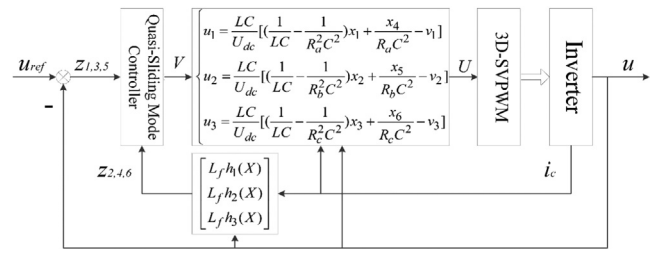

Fig. 13. Block diagram of the control strategy for a four-leg inverter presented by Yang et al.

the pole assignment method. On the other hand, the control system for the latter case is nonlinear. Based on the state variable feedback equations and (10), the variable structure can be transformed into the original system to design the control scheme. The proposed control strategy is shown in Fig. 13.

3.2. Stationary αβo reference frame control structure

The reference frame with v_α, v_β and v_o as coordinates referred to as the stationary reference frame [20]. The voltages/currents in the abc frame can be transformed into the stationary reference frame using the Clarke transformation [20,21]. As the control variables are time-varying in this structure, classical PI controllers face difficulties to obtain zero steady-state error. Recently, more attention has been paid to the use of PR controllers in the αβ0 reference frame due to their superior performance characteristics in eliminating the steady-state error and capability to compensate multiple harmonics [26]. In this part, available approaches for the control of four-leg VSIs operating in autonomous mode in the stationary reference frame are presented.

3.2.1. Available control techniques for four-leg VSI in the stationary αβo reference frame

The idea introduced by Li et al. [62], proposes a grid-interfacing power quality compensator using three-phase four-leg inverters for a four-wire microgrid. The microgrid can operate in both grid-connected and islanded modes. The proposed control method is partly similar to the series-parallel active filter [63]. Indeed, one inverter is connected to the microgrid in shunt structure, while the second is in series with the microgrid. Whenever a power quality event or an external attack occurs within the utility grid, the shunt converter A operates as an UPS to support the critical load. On the other hand, the series converter B can compensate the harmonic voltage components in grid-connected mode to improve the power quality of the system.

The control scheme of the shunt inverter is exhibited in Fig. 14. It is apparent from this figure that the deviations of power angle and voltage amplitude are utilized to control the output active and reactive power of the shunt inverter. As seen, the reference voltages of the proposed controller are provided in the stationary frame. Three independent dual-loop controllers in positive, negative and zero-sequence are employed to properly track the reference voltages. The proposed control scheme includes an outer voltage loop for voltage regulation and an inner current loop for current adjustment. The positive and negative-sequence voltages are regulated using the stationary reference frame equivalent of reference frame approach [64]. This approach significantly simplifies the stability analyses and control parameter design. However, the zero-sequence voltage controller operates independently from the others in the stationary reference frame.

Two PI compensators are used for positive and negative-sequence voltage controllers, while the zero-sequence voltage is implemented using a P+resonant compensator. The inner current

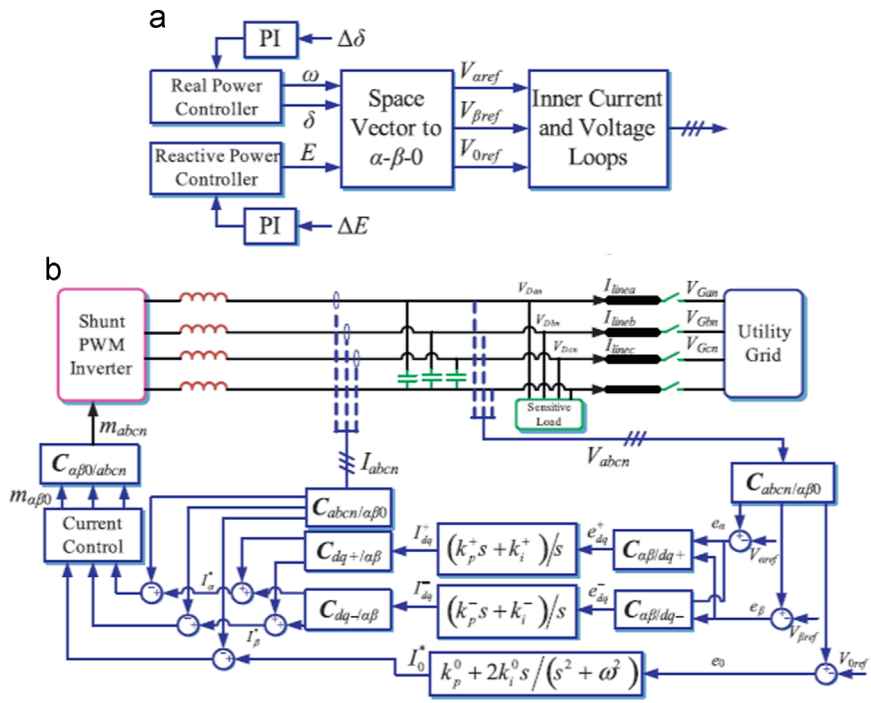

Fig. 14. Control strategy for shunt inverter A. (a) overall control structure and (b) voltage control algorithm.

loops are also designed in three channels using a simple proportional gain in the stationary reference frame. The series inverter is also implemented using an external current loop and an internal voltage loop. Two PI compensators in the dq frame are used in the outer loop to generate the voltage references for the inner voltage loop. A PR controller is also adopted for the current loop in the 0-axis to compensate zero sequence current.

The work by Rokrok and Hamedani [65], presents an improved control strategy for a four-leg VSI operating in stand-alone mode to provide high-quality AC output voltages under unbalanced and nonlinear load conditions. The structure of the proposed control strategy is depicted in Fig. 15. As can be observed, the control scheme is implemented in the stationary frame in three different channels. For each direction in the αβo frame, there exists an independent controller to accurately track the reference signals. As seen, two nested loops and a feed-forward path are used in each control direction to meet the power quality requirements under unbalanced and nonlinear load conditions. The cascaded loop comprises an internal current controller and an external voltage loop to compensate the voltage and current within standard values.

The inner current loop is designed using the state feedback approach. It is responsible for the protection of the inverter against overload and enhancement of the control system robustness [66]. The reference of the current loop is generated using the voltage controller and the feedforward current control path. A limiter block is also employed in the reference current path to limit the inverter output current to a certain level. The voltage loop is implemented using PR controllers to provide an infinite gain at the fundamental frequency and track the reference command. The feedforward path is also employed in the outer loop to attenuate the effects of load disturbances on the output voltages of the inverter by decreasing its output impedance. The PR controller is able to compensate for the low-order harmonics effectively (Fig. 15).

A grid-interfacing converter system for power quality improvement in amicrogrid applications is proposed in [67]. The main aim of this study is to provide a suitable voltage quality for

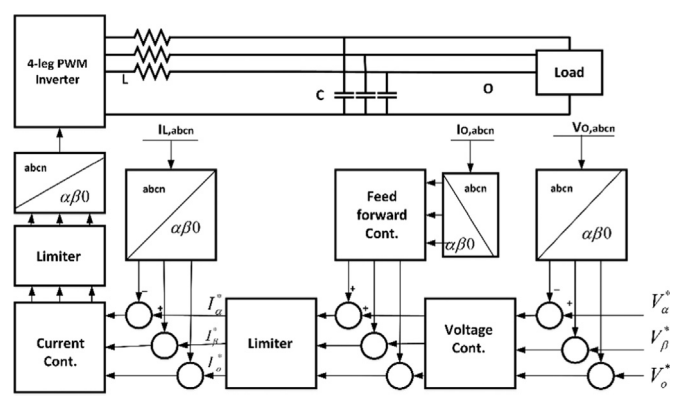

Fig. 15. Block diagram of the control strategy proposed in [65].

the critical loads and to enhance the power quality at the grid side. The configuration of this system is shown in Fig. 16. As seen, it includes two different levels. The purpose of the first level is mainly voltage quality enhancement for the local loads within the system module, and bidirectional energy transfer under disturbed grid conditions. Specifically, the parallel converter works as a voltage source so as to provide balanced and sinusoidal voltage under asymmetrical and nonlinear load conditions. As a benefit, it can easily switch to the islanding mode and offer uninterruptible service when the grid voltage interrupts. Power flow control can be achieved by the series converter.When disturbances appear in the grid voltage, the module can still deliver power between the grid and the local system. On the other hand, the series–parallel system can act as an active filter to prevent low-order current harmonics from flowing through the utility grid, while higher-order harmonic currents can be easily removed by adding passive filters if necessary.

The block diagrams of the proposed controller for the parallel converter is depicted in Fig. 17. To obtain an excellent steady-state feature, the PR controllers $G_{c,\alpha\beta\gamma}(s)$ are employed for the parallel converter. Besides, the transfers $F_{i\alpha\beta\gamma}(s)=K_{fi}s/(s+2\pi f_{hp})$, are

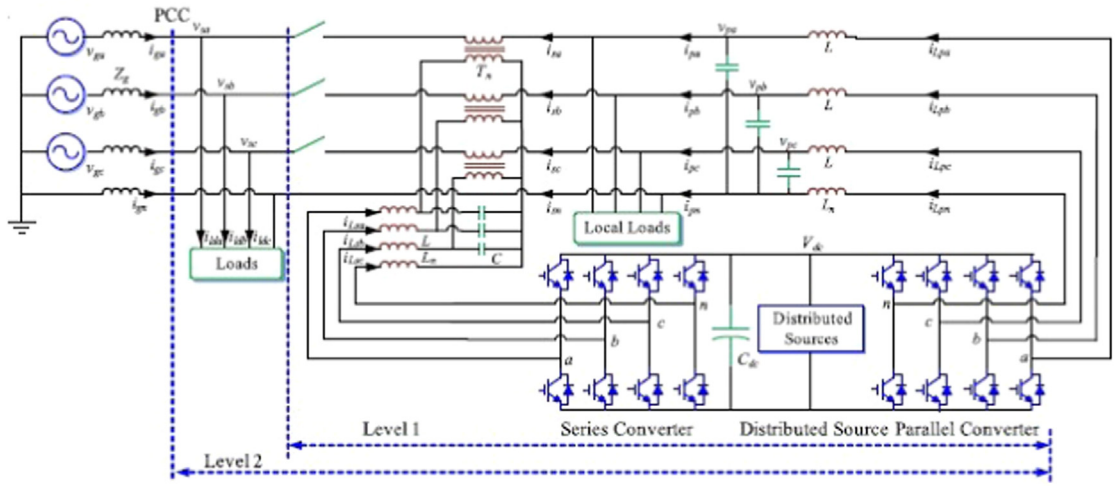

Fig. 16. Configuration of the system presented in [67].

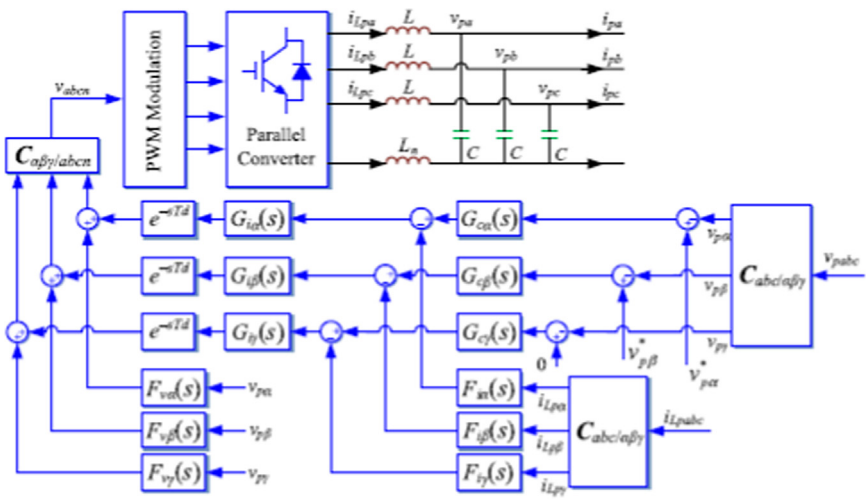

Fig. 17. Control diagram of the parallel converter in [67].

employed to enhance the disturbance sensitivity of the system. Furthermore, $F_{i\alpha\beta\gamma}(s) = K_{ff}e^{-Td}$ is transfer delay function, where K_{ff} denotes the forward gain. Similarly, the control scheme of the series converter is presented in Fig. 18. It should be noted that a weighted currents feedback control approach is utilized to reduce the third-order LCL-filter model as a first-order one [68].

The proposed approach presented in [69], is fundamentally same as mentioned in [65]. This approach proposes a dual-loop control strategy using the interleaving method for paralleled three-phase four-leg VSIs. The control scheme is implemented in three independent channels using the αβo reference frame. The structure of the suggested scheme in each channel is illustrated in Fig. 19. It includes a proportional inner current loop to achieve a fast response for tracking the current command, a PR voltage controller for voltage regulation and a state observer for improving the stability of the system. Note that the inductor current is chosen as a feedback signal in the inner current loop. Since there is one step-delay between the voltage command and the inverter terminal voltage, the stability of the whole system may be jeopardized. Hence, the state observer is utilized to predict the output voltage and inductor current in the next time step. It is designed based on the space model of the three-phase four-leg VSI in the stationary reference frame. The state space model of the system in the continuous-time domain can be obtained as:

$$\begin{cases} \dot{x} = A_n x_n + B_n V_{in} + N_n I_{On} \\ y_n = C_n x_n \end{cases} \tag{11}$$

where $x_n = \begin{bmatrix} V_n & I_n \end{bmatrix}^T$, $C_n = \begin{bmatrix} 1 & 0 \end{bmatrix}$, $A_n = \begin{bmatrix} 0 & \frac{1}{C} \\ \frac{-1}{L_n} & \frac{-r_n}{L_n} \end{bmatrix}$, $B_n = \begin{bmatrix} 0 \\ \frac{1}{L_n} \end{bmatrix}$ and $N_n = \begin{bmatrix} \frac{-1}{C} \\ 0 \end{bmatrix}$. L_n and r_n are the equivalence inductance and resistance in each channel. The discrete state space model of the system is obtained using the ZOH approach. Afterwards, the predict error of the sate observer is presented as:

$$\hat{x}_n(k+1) - x(k+1) = (A_{nd} - H_{nd}C_{nd})\left[\hat{x}_n(k) - x_n(k)\right] \tag{12}$$

where A_{nd}, B_{nd} and N_{nd} are state matrix of the system in the discrete time domain. H_{nd} is also the feedback matrix. It is used to eliminate the predictive error of the state observer. This observer can effectively estimate the voltage and current in the next-time step.

3.3. Synchronous dqo reference frame control structure

The synchronous dqo reference frame is one of the well-known control structures for control of power electronic inverters in

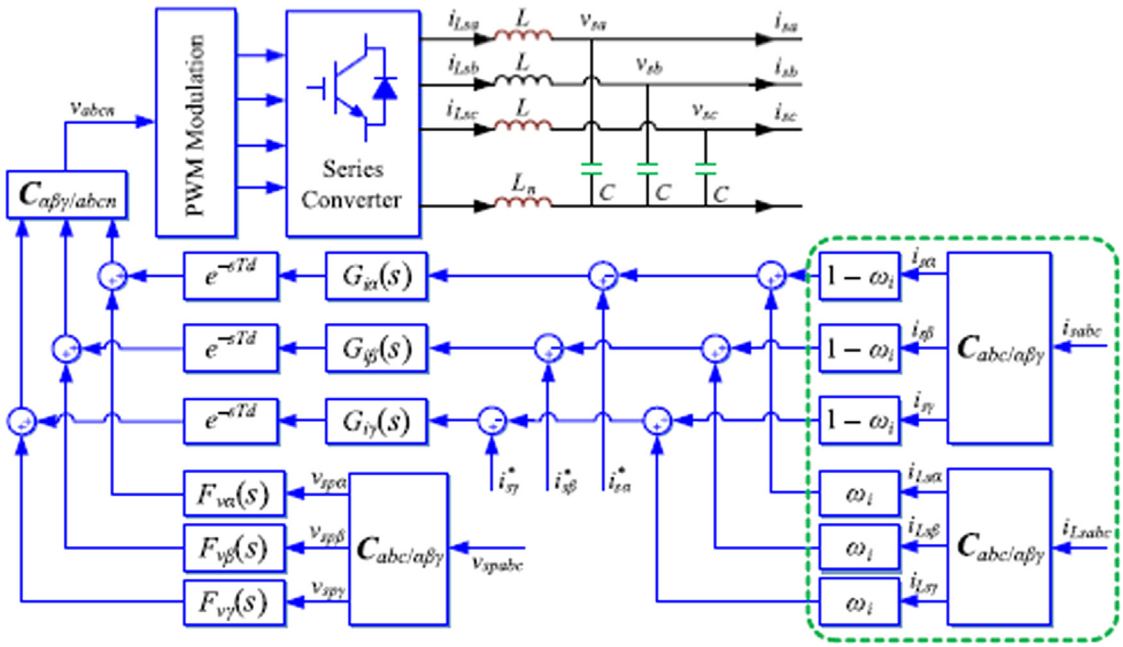

Fig. 18. Control diagram of the series converter in [67].

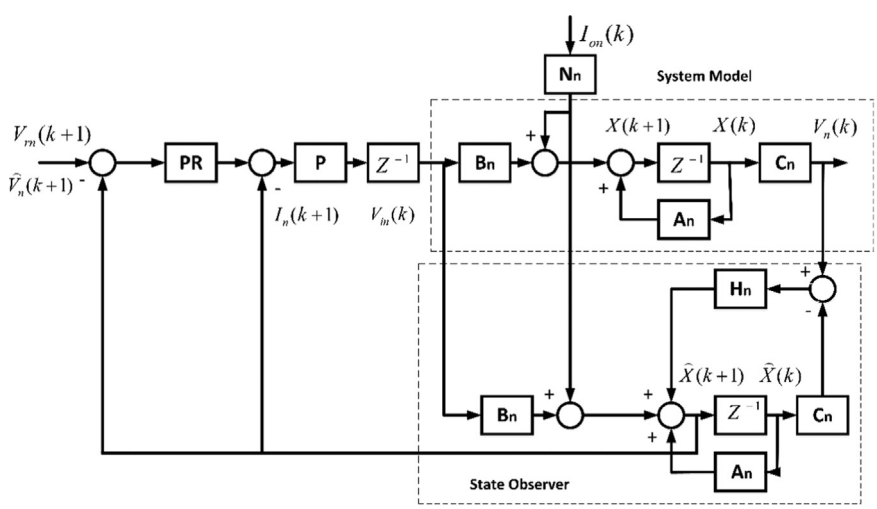

Fig. 19. Control scheme presented by Lei et al.

renewable energy and smart grid integration [4]. It can be implemented by transferring the three-phase control variables into direct–quadrature–zero components [20]. Since this reference frame rotates with the grid voltage synchronously, it is no longer a function of time. It is accomplished through applying the Park transformation [21]. The synchronous dqo reference frame facilities the controller design and analysis because all AC quantities become DC quantities.

3.3.1. Available control techniques for four-leg VSI in the dqo reference frame

In [70], using a combination of the synchronous and stationary frame control structures, an improved control scheme proposed for a four-leg VSI to compensate the distorting effects of nonlinear and unbalanced loads. Typically, the d- and q-components of a three-phase balanced system are DC quantities, and the o-component is zero. However, under the unbalanced condition, the d- and q-components include an additional AC quantity. Furthermore, the o-component is not zero and oscillates with the same frequency as the output voltage [20]. To cope with this challenge, this paper uses the dq frame control structure to compensate the positive and negative sequence distortions, while the stationary frame control structure is employed to eliminate the zero sequence distortions caused by unbalanced and nonlinear loads.

The suggested control strategy for unbalanced load compensation is shown in Fig. 20. The proposed controller contains three distinct controllers to generate purely fundamental output voltages. A positive and a negative synchronous frame integral compensator rotating at the fundamental frequency are used to respectively attenuate the positive and negative distortions caused by unbalanced loads. A zero sequence stationary frame regulator is also employed to compensate the zero sequence component. Indeed, a zero-damping band-pass filter with the resonant frequency of w is added as a parallel path to the o-channel of the controller to provide an infinite gain at the zero sequence disturbance frequency. The proposed control scheme for nonlinear load compensation is also presented in Fig. 21. Similarly, it is implemented in three different channels with same reference frame and controllers. However, the positive and negative

synchronous frame integral controllers are responsible for compensation of $[(6 \cdot n)+1]$. w harmonic frequencies caused by diode rectifiers. The odd triplen harmonics (3rd, 9th, etc.) produced by single-phase diode rectifiers are also eliminated through the zero sequence stationary frame controller. The proposed controller has the proper ability to compensate for unbalanced and nonlinear loads. However, the effectiveness of the proposed scheme is only presented for the steady-state condition, and the zero steady-state error for the zero sequence component is not truly achieved.

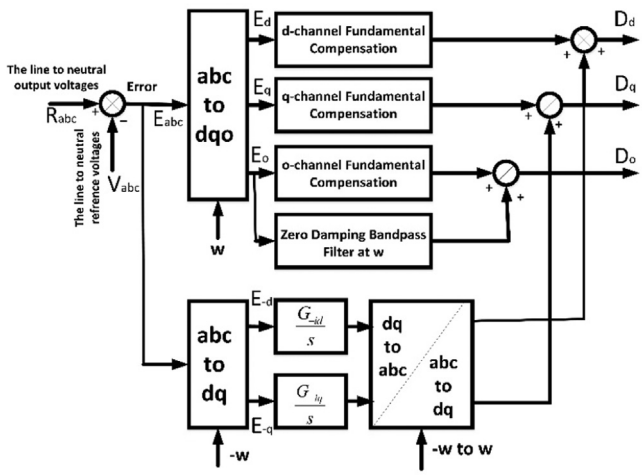

Fig. 20. Proposed control structure for unbalanced load compensation in [70].

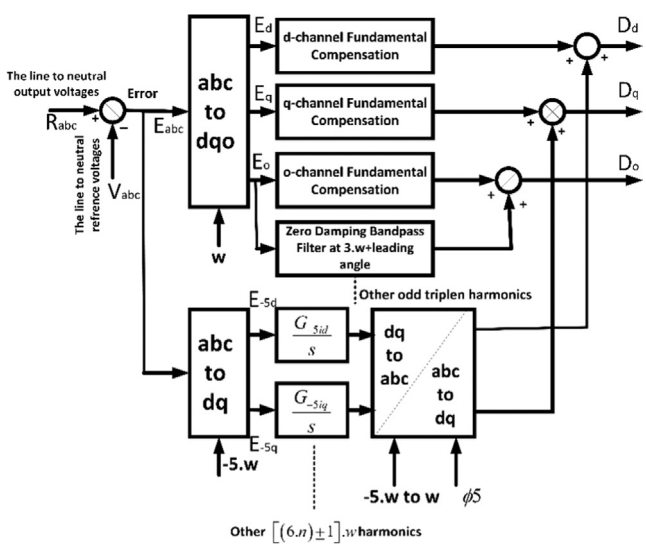

Fig. 21. Proposed control structure for non-linear load compensation in [70].

The idea presented by Yi and Jin [71], introduces a control approach in the dqo frame for a three-phase four-leg inverter power supply. This method is proposed to compensate voltage distortions caused by unbalanced loads. The block diagram of the control scheme is illustrated in Fig. 22. As seen, the proposed control strategy is implemented using an inner current loop and an outer voltage loop in three different channels in the synchronous reference frame. The voltage loop uses the PI controller to regulate output voltages, while the inner current loop utilizes the P compensator to provide an accurate command for the PWM. Moreover, two capacitor current feedforward loops are employed to mitigate the cross-channel coupling of the dq channels bringing from capacitances. In other words, the capacitor current reference feedforward value $-wCV_q^*$ to d-channels can compensate d-channels coupling item. In the same way, the capacitor current reference feedforward value $-wCV_d^*$ to q-channels can compensate q-channels coupling item. This method has good dynamic characteristics.

Over the past decade, most research in control of four-leg VSI has emphasized the use of Symmetrical Components Calculators (SCCs) to compensate unbalanced loads [72–75]. In this approach, first the symmetrical components of the unbalanced voltages and currents are derived, and then they transfer into the dqo reference frame. This method operates based on all-pass filters to provide zero steady-state error. Based on the SCC strategy, Vechio et al. [72], describe two control strategies for a four-leg VSI operating in a transformerless HPS. The first approach is designed based on the classical current–voltage controller, whereas the second method is implemented using the SCC. Firstly, the mathematical model of the four-leg inverter is obtained using the average technique as shown in Fig. 23. The voltage equation of the average model in the dqo frame is explained as follows:

$$\begin{bmatrix} v_{fd} \\ v_{fq} \\ v_{fo} \end{bmatrix} = \begin{bmatrix} v_d \\ v_q \\ v_o \end{bmatrix} + R_f \begin{bmatrix} i_d \\ i_q \\ i_o \end{bmatrix} + L_f \frac{d}{dt} \begin{bmatrix} i_d \\ i_q \\ i_o \end{bmatrix} + L_f w \begin{bmatrix} -i_q \\ i_d \\ 0 \end{bmatrix} - R_N \begin{bmatrix} 0 \\ 0 \\ -3i_o \end{bmatrix} - L_N \frac{d}{dt} \begin{bmatrix} 0 \\ 0 \\ -3i_o \end{bmatrix}. \tag{13}$$

where $i_d, i_q, i_o, v_{fd}, v_{fq}, v_{fo}$ and v_d, v_q, v_o are the line currents and output voltages before and after the inverter filter in the synchronous reference frame. Afterwards, using the obtained model two different control schemes are proposed. Finally, the authors critically compare the main characteristics of these two methods.

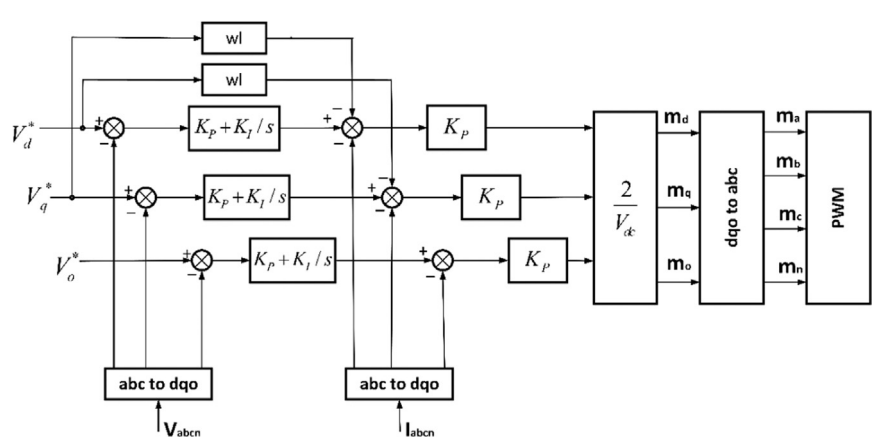

Fig. 22. Block diagram of the control scheme presented by Yi and Jin.

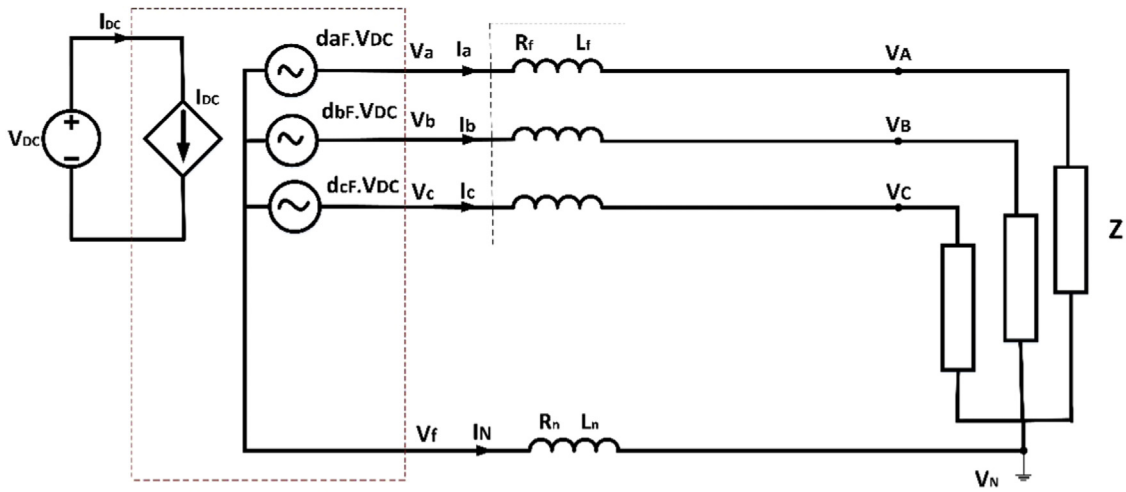

Fig. 23. Average large signal model of the four-leg inverter.

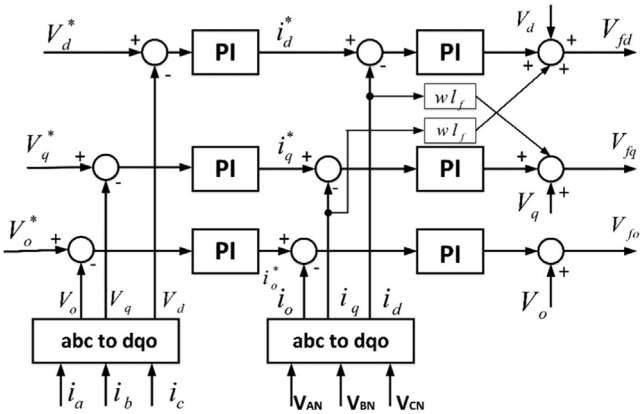

Fig. 24. Control strategy based on the classical current–voltage controller presented by Vechiu et al.

Fig. 24 indications the block diagram of the proposed control strategy based on the conventional dqo frame. It is designed in three-channel arrangement based on the transformation of the three-phase voltages and currents into the dqo frame. It contains an outer voltage loop and an inner current loop in each channel. The PI controller is employed in both control loops to ensure voltage and current regulation. Since the d- and q-components are coupled through $L_f w i_q$ and $L_f w i_d$, decoupling terms are also used to decouple these channels. Based on (13) the o-channel is fully decoupled from the d and q channels.

The second strategy is proposed on the basis of decomposition of three-phase voltages and currents into instantaneous positive, negative and homopolar sequence components as depicted in Fig. 25. In this scheme, the unbalanced voltages and currents are decomposed into symmetrical components so that the control variables can be adjusted independently in three different sequence components. The first channel controls the positive sequence of voltages and currents in the dqo frame, while the second channel regulates the negative sequence of voltages and currents. The third channel also compensates the homolpolar voltages and currents. Similarly, the conventional PI regulators are applied to regulate the voltage and current loops. The second method shows better performance compared with the former. It is because of the fact that the independent control in three different sequence components provides superior performance to compensate for the unbalanced loads.

The transient operation of the latter approach is also investigated using experimental results in [73]. Cárdenas et al. have recently developed the idea of the SCC using the combination of synchronous and stationary frame control strategy for a four-leg matrix converter in [74]. The suggested scheme includes d–q controllers implemented in the synchronous frames to compensate the positive and negative components of the load voltage. Indeed, a vector control system based in two synchronous rotating d–q axes is used to regulate the load voltage. The frames are rotating clockwise and counter-clockwise respectively in order to control the positive and negative sequence of the output signals. A separate resonant controller is also used to regulate the homopolar components of the load voltage.

An improved SCC control strategy using an isochronous control function for a grid-forming four-leg VSI in a four-wire system is presented in [75]. The isochronous control approach is a special droop controller (zero droop), whose concept is inherited from the synchronous generators in conventional power systems. Fig. 26 illustrates the isochronous function for an inverter operating at the same frequency and voltage regardless of the load. Although the implementation of this load sharing approach needs communication links, it provides appropriate voltage and frequency control for the inverter. The proposed scheme compensates each sequence component separately in the dqo frame. The block diagram of the proposed control scheme for the positive sequence component is presented in Fig. 27. First of all, the positive, negative and zero sequence active/reactive power consumption by the load $(P_{total+,-,0}, Q_{total+,-,0})$ and active/reactive power generation via the inverter $(P_{Gen,n,+,-,0}, Q_{Gen,n+,-,0})$ are calculated. Subsequently, the total measured active power in each sequence is divided by the total rated power, and compared to the respective sequence generated active power divided by its rated power:

$$\Delta P_{+,-,0}\% = \frac{P_{total+,-,0}}{S_{total}} - \frac{P_{Gen,n,+,-,0}}{S_{Gen,n}} \tag{14}$$

The difference obtained from (14) is magnified using a P-factor that is tuned from the dispatcher in the superordinate management level. Afterwards, this signal is added to the summation point of the reference angular frequency in the q-component. Similarly, the reactive power can be controlled in each sequence separately. Indeed, the total measured reactive power consumption is divided by the total rated power, and then it is compared to the active power supplied by the four-leg VSI divided by its rated

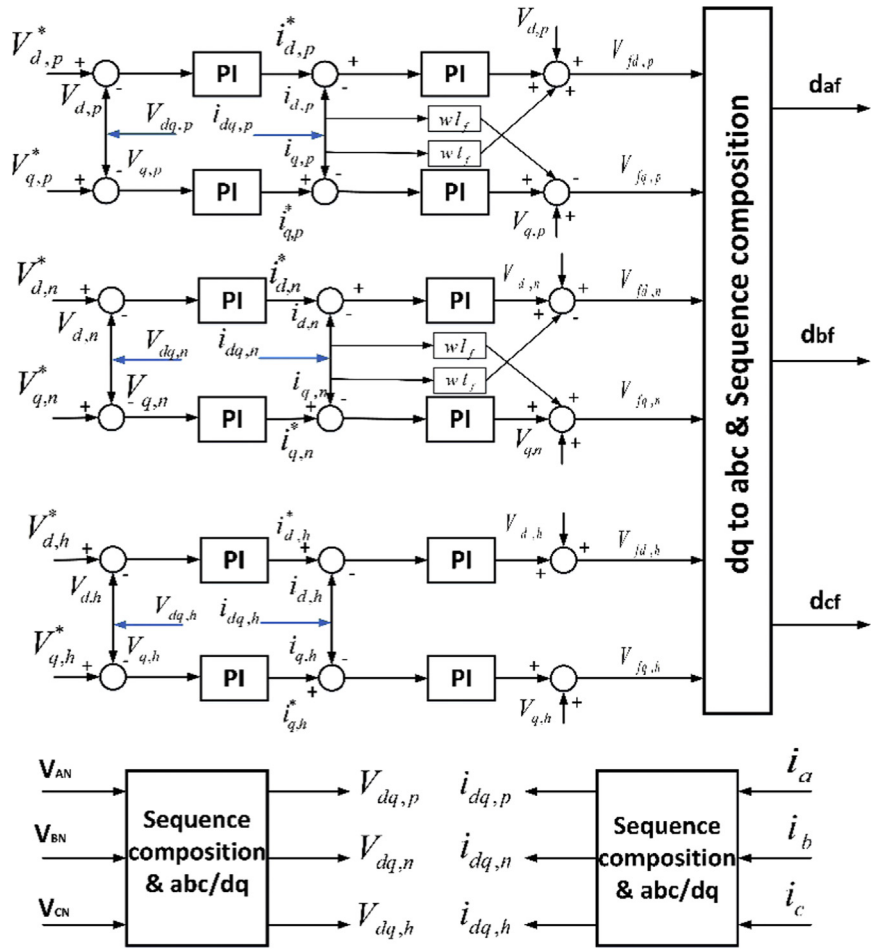

Fig. 25. Control strategy based on the SCC approach presented by Vechiu et al.

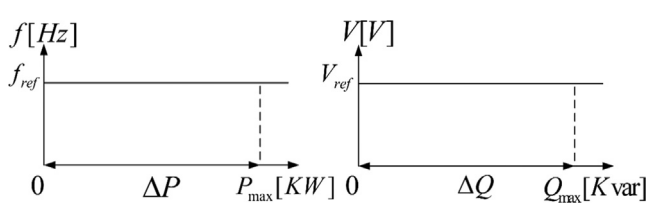

Fig. 26. Frequency versus active power and voltage versus reactive power (isochronous function).

power:

$$\Delta Q_{+,-,0}\% = \frac{Q_{total+,-,0}}{S_{total}} - \frac{Q_{Gen,n,+,-,0}}{S_{Gen,n}} \tag{15}$$

A Q-factor is also used for the reactive power controller to amplify the difference obtained from (15). Moreover, it is added to the summation point of the reference angular frequency in the d-component. Two nested loops for each sequence are used to regulate the voltages and currents in the synchronous reference frame. The output signals from the isochronous control function are passed to the voltage controllers to compare to actual voltage values. Subsequently, the output of each voltage controller is fed to a current controller to generate the switching states.

An innovative control method on the basis of the Proportional Integral Derivative (PID) voltage controller is presented in [76] to compensate unbalanced and nonlinear loads. The block diagram of the proposed approach is shown in Fig. 28. As seen, it is implemented using an external PID voltage regulator. An output voltage feedback inner loop is also added to the control structure to enhance the dynamic and static performances of the system. Additionally, it has the ability to curb the impact of load disturbances. The internal loop is implemented using the PD regulator. The control procedure is accomplished by extracting the average model of the four-leg inverter in the dqo reference frame and designing the control parameters using the pole-assignment approach.

In [77], a state feedback control strategy is offered for a four-leg inverter used for the high speed permanent magnet generator driven by a micro-turbine. The block diagram of the system, including the inverter is illustrated in Fig. 29. The main responsibility of the four-leg inverter is to provide balanced output voltages under unbalanced load condition. Based on the state feedback control strategy, a pole assignment approach on the basis of the system matrix is suggested to compensate for the asymmetrical voltages. First of all, the average model of the four-leg inverter is derived. Subsequently, considering the output phase voltage as the state variable, the state equations of the four-leg inverter in the dqo frame are expressed as:

$$\begin{bmatrix} I_d \\ I_q \\ I_o \end{bmatrix} = \begin{bmatrix} CP & -wC & 0 \\ wC & CP & 0 \\ 0 & 0 & CP \end{bmatrix} \begin{bmatrix} V_d \\ V_q \\ V_o \end{bmatrix} + \begin{bmatrix} I_{L-d} \\ I_{L-q} \\ I_{L-o} \end{bmatrix} \tag{16}$$

where I_{dqo}, C, I_{L-dqo} and P denote the inductor phase currents, the filter capacitance, the load currents and differential operator, respectively. Next, using the small signal analysis the matrix transfer function of the system is presented. It is obtained by neglecting the cross-coupling between the system's output and input. Finally, based on the state feedback control strategy, the

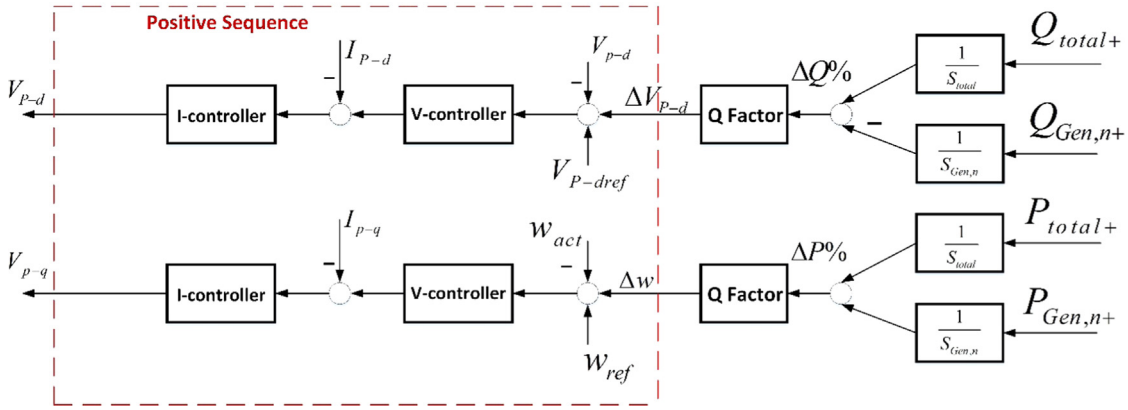

Fig. 27. Block diagram of the control strategy proposed by Sinsuthavorn et al.

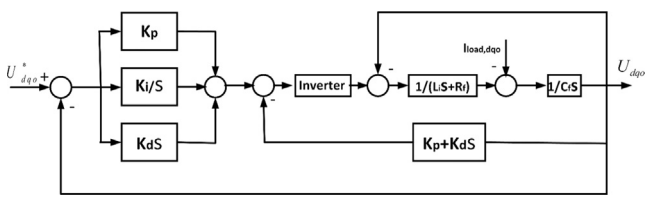

Fig. 28. Block diagram of the four-leg control system with PD feedback inner loop presented by Liu et al.

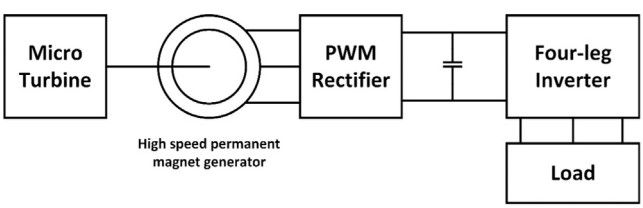

Fig. 29. Schematic diagram of the system presented in [77].

pole assignment approach is used. The proposed method shows accurate transient and steady-state performance. However, the structure of the controller is relatively complicated.

An adaptive pole-placement control approach via state feedback is proposed in [78]. This approach is suggested for a four-leg VSI operating in a stand-alone photovoltaic system to generate a balanced voltage in the presence of unbalanced loads. The average large-signal model of the four-leg inverter is used in order to design this modern control. Since the implementation of this control strategy needs a DC operating point, the average model of the system is transformed into the synchronous reference frame. It is assumed that the load is balanced *RL* time-invariant. Additionally, by neglecting the coupling effects between d and q channels, the independent control of the system is provided. The average model of the four-leg inverter in the dqo frame is presented in Fig. 30. The state-space equations of the model presented in the synchronous frame are derived for each channel independently.

The pole-placement control strategy via state feedback and a static lead compensator is then used in each channel as shown in Fig. 31. In this Figure, r is a vector with one input, K is the state feedback, and G is the static lead compensator. Considering that the controller has the linear state feedback form ($u=-k.x+G.r$), K and G are the unknown controller matrixes with dimensions 1×3 and 1×1, respectively. The main aim is to find the unknown matrixes such that the closed-loop system can be achieved the desired objectives. The pole-placement method is adopted in order that the poles of the closed-loop system obtain desirable pre-assigned values. Finally, a Self-tuner Regulator (STR) is

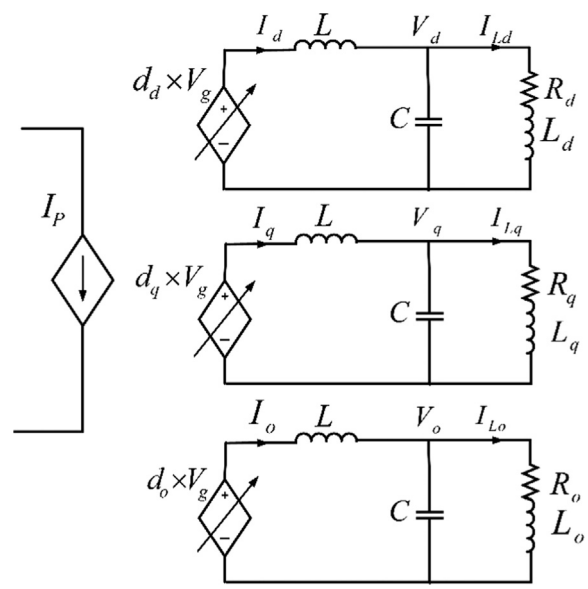

Fig. 30. Average mode represented as signal flow graph.

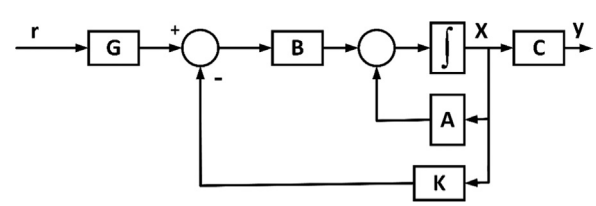

Fig. 31. Block diagram of the pole-placement control strategy via state feedback presented by Nasiri and Radan.

presented to ensure the performance of the proposed scheme in the presence of time-variant loads. The suggested STR is depicted in Fig. 32. The major task of the STR is to tune the feedback vector using the calculation of the K and Gmatrixes. Initially, the current and voltage of the load are sampled. After that the parameters of the load are determined and feed to the STR. This strategy provides an adaptive operation for the final system.

The idea promoted by Ninad et al. [79,80], presents an improved per-phase control technique for a four-leg grid-forming VSI to provide balanced output voltages under highly unbalanced load condition. The structure of the suggested control scheme for the a-phase is presented in Fig. 33. This method uses the concept of fictive axis emulation to create an orthogonal component from the original signal to control the voltage phases independently. This controller is implemented in three different channels in the

dq frame. The control system consists of an inner current loop, an outer voltage loop and several feedforward paths in each phase. The main function of the external voltage loop is to control the instantaneous output voltages within the standard limits. The inner current loop is adopted to generate the switching states of the PWM modulator after compensating the error between the reference signal and the actual measured signal. Feedforward loops are also employed to decouple the d and q channels from each other. It is noteworthy that the inductor current is employed as the feedback signal in the inner loop. However, to achieve a very fast response, the orthogonal current component (I_β) is obtained by emulating a fictive circuit as depicted in Fig. 33, in dotted lines.

Both the voltage and current loops operate in the synchronous reference frame. In the outer loop, V_{ca} is the a-phase output voltage of the filter capacitor to neutral line. V_α and V_β are the real and the orthogonal components of the V_{ca} in the stationary reference frame, respectively. The orthogonal component is obtained using the Second Order Generalized Integrator (SOGI) technique. The dq components of the a-phase output voltage of the filter capacitor can be generated by applying the Park transformation, after creating the pseudo-two-phase system. A simple Phase-locked loop (PLL) is also used to obtain the $\sin\theta$ and $\cos\theta$ terms. The PI controllers are utilized in the voltage loop to regulate the instantaneous output voltages in the dq frame because of its superior performance in obtaining zero error in steady state and fast transient response when signals are pure DC. The reference voltages for the three phases have equal amplitudes, but are separated from the other voltages by a phase angle of 120°. The q-component of the reference voltages in each phase (V_q^*) is set at 0, whereas the d-components (V_d^*) is set at the peak value of the reference phase voltage. The inner current loop in each phase also compares the reference current generated by the voltage loop and the measured current using the PI controller to generate the switching states of the PWM.

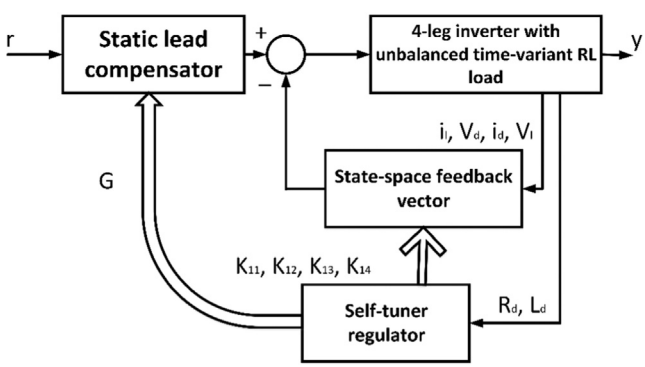

Fig. 32. Self-tuner regulator presented in [78].

4. Comparative analysis and suggestions for the future research

Four-leg VSIs are special DC to three-phase AC converters, whose control strategies can relatively inherit from the three-phase three-leg power inverters. The control strategies of four-leg VSIs in autonomous mode can be classified in several categories based on different consideration as shown in Table 2.

From the view of modulation, the control schemes of four-leg VSIs can be broadly classified as two categories, namely carrier-less modulations and carrier-based modulations. The carrier-less modulation methods such as hysteresis and flux vector provide a fast dynamic response [81]. Nevertheless, they suffer from variable switching frequency [44]. Additionally, they use complex switching tables. In contrast, the carrier-based approaches such as Sinusoidal Pulse Width Modulation (SPWM), 3D SVPWM, Minimum Loss Discontinuous PWM (MLDPWM) and Selective Harmonic Elimination (SHE) based PWM have received considerable attention because of their constant switching frequency [82]. The SPWM provides flexible control schemes and constant switching frequency; however, one major drawback of this approach is the low efficiency of DC voltage [19]. The 3D SVPWM provides an acceptable DC bus utilization and an adequate load harmonic profile than the SPWM. Nonetheless, it is complicated in nature to implement on digital devices. Similarly, the SHEPWM offers flexible control approach using the switching angle. However, the real-time implementation of this carrier-based modulation is relatively complicated. The performance of the MLDPWM under unbalanced and nonlinear conditions is suitable; however, its real-time implementation is highly complicated.

From the view of the reference frame control structure, the control of four-leg VSIs in autonomous mode can be designed in three coordinate systems. As mentioned before, the nonlinear controllers such as the hysteresis and sliding mode control are preferred to operate in the natural abc frame because of their high dynamic [20]. The PR controller is also can be easily implemented in this reference frame. Since the neutral connection is provided in four-leg VSIs, the control matrix of the PR controller no need to use cross-coupling terms [21]. However, the use of the PI controller is

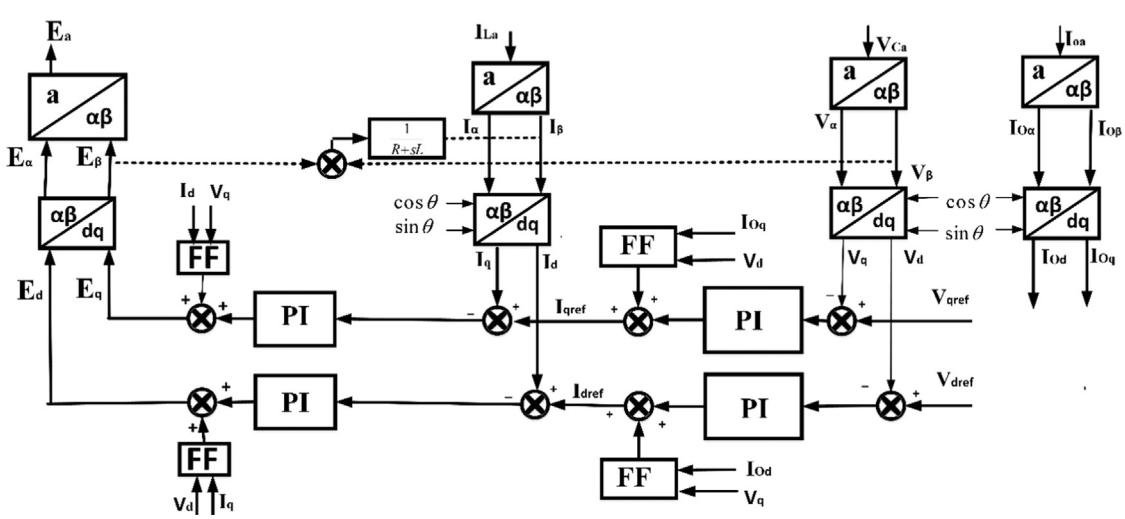

Fig. 33. Schematic diagram of the per-phase control strategy proposed by Ninal et al.

Table 2
Comparison of different control strategies for four-leg VSI in autonomous mode.

Reference	Reference frame	Control method	Modulation	Ancillary services	Type of utility
[40,41]	The abc frame	P+resonant-filter bank	MLDPWM	Voltage unbalanced/harmonic compensation	UPS
[44]	The abc frame	Hysteresis	Hysteresis	Voltage unbalanced/harmonic compensation	Stand-alone DG, UPS
[48]	The abc frame	Repetitive	3D SVPWM	Voltage unbalanced/harmonic compensation	Variable speed generation system
[50]	The abc frame	PR voltage control and P current control	SPWM	Voltage unbalanced/harmonic compensation, unbalanced/harmonic power sharing	Autonomous microgrid
[31,57,58]	The abc frame	Predictive	–	Voltage unbalanced/harmonic compensation	Stand-alone DG, UPS
[61]	The abc frame	Sliding mode control via state feedback	3D SVPWM	Voltage unbalanced/harmonic compensation	Stand-alone DG, UPS
[62]	The stationary frame	PR and PI voltage control and P current control	SPWM	Voltage unbalanced/harmonic compensation	Microgrid, UPS
[65,66]	The stationary frame	The PR voltage and current controller	SPWM	Voltage unbalanced/harmonic compensation	Stand-alone DG, UPS
[67]	The stationary frame	PR	SPWM	Ride through voltage disturbances, Voltage unbalanced/harmonic compensation	UPS, microgrid
[69]	The stationary frame	PR voltage control and P current control	SPWM	Voltage unbalanced compensation	Paralleled four-leg VSIs
[70]	The dqo frame and the stationary frame	Integral control and the zero-damping band-pass filter	3D SVPWM	Voltage unbalanced/harmonic compensation	Stand-alone DG
[71]	The dqo frame	PI voltage control and P current control	SPWM	Voltage unbalanced compensation	Stand-alone DG
[72,73]	The dqo frame	PI voltage control and PI current control	3D SVPWM	Voltage unbalanced compensation	HPS
[74]	The dqo frame	PI and resonant control	3D SVPWM	Voltage unbalanced compensation	Stand-alone DG
[75]	The dqo frame	PI voltage control and PI current control	3D SVPWM	Voltage unbalanced compensation	Autonomous microgrid
[76]	The dqo frame	PID and PD voltage control	SPWM	Voltage unbalanced/harmonic compensation	Stand-alone DG
[77]	The dqo frame	State feedback control	3D SVPWM	Voltage unbalanced compensation	Stand-alone DG
[78]	The dqo frame	Pole-placement control	–	–	Stand-alone DG
[79,80]	The dqo frame	PI voltage control and PI current control	SPWM	Voltage unbalanced compensation	HPS

far from straightforward in this coordinate system due to the complexity of the controller matrix. Indeed, that is because of the cross-coupling terms between the phases in four-wire systems [20]. Some novel control strategies such as the repetitive and predictive control are also used for control of four-leg VSIs in this coordinate system.

The control variables are time-varying waves in the stationary frame. Therefore, the classical PI controller encounters a problem to eliminate the steady-state error. The PR controller in the stationary reference frame has been commonly used for controlling the output voltages of the four-leg inverter due to its superior performance in eliminating the steady-state error, while regulating sinusoidal signals. Moreover, it has a great ability to eliminate selective harmonic disturbances. It should be noted here that the PR controller uses the information of the resonant frequency to provide gains at certain frequencies. Hence, the resonant frequency must be identical to the frequency of the autonomous microgrid. In other words, it is greatly sensitive to system frequency variations. The PI controller in the dqo frame is also widely used and works well with pure DC signals. However, in order to transfer the control variables from the abc frame to the dqo frame the phase angle of the autonomous microgrid is a must. Moreover, the use of voltage feedforward and cross-coupling terms are other problems with this approach.

In autonomous operation, VSIs are mainly responsible for transferring power and controlling the voltage and frequency of the system. However, power quality enhancement can be achieved by presenting a proper control scheme, when the DGs are of inverter-based type. Since four-leg inverters are the voltage source type, the ancillary services for power quality improvement on voltage issues can be easily embedded in their control scheme. From the view of auxiliary functionalities of four-leg VSIs in power quality enhancement, unbalanced voltage compensation, harmonic voltage compensation, active/reactive power sharing, reactive power, imbalance power, and harmonic power sharing schemes are embedded in the control strategies. However, since from the view of the type of autonomous system, most of the control strategies are proposed for single-bus stand-alone microgrids, UPSs and HPSs, the power-sharing issues are not perfectly investigated in the previous studies.

Moreover, a comparison among all studied voltage control techniques is presented in Table 3. This comparative study lists the benefits and drawbacks for each controller in terms of robustness against parameter variation, rapidity, stability, harmonic elimination, unbalanced compensation and nonlinearity of the system. As mentioned before, various suitable control strategies for three-phase four-leg VSIs operating in autonomous microgrids have been documented in the literature. Nonetheless, their operations for power generation and power quality improvement at the same time are still not perfect. Additionally, most of them are proposed for autonomous systems with a DG and small capacity. Besides, each controller has its own strength and limitation. Hence, it is hard to say which control scheme is better than the others. These are important issues for future research. Based on the analysis of previous publications, further research is recommended to be conducted in the following area:

- In spite of the numerous investigations have been done in this field, none of the used control techniques can be elected as a perfect solution to compensate all the power quality requirements such as voltage unbalanced/harmonic/interruption/sag/swell compensation and reactive/imbalance/harmonic power sharing at the same time. Future research should therefore concentrate on the novel power electronic topologies to fulfill all the mentioned requirements at the same time.
- The Hierarchical control of three-phase three-wire microgrids is now a mature and well-developed research topic. However, for

Table 3
Advantages and disadvantages for each voltage controller.

Method	Advantages	disadvantages
Hysteresis control	It is very simple and robust, bring extremely fast transient response and its implementation does not require complex circuits.	Variable switching frequency and high current ripple are the main limitations with this approach. The switching losses restrict the application of hysteresis control to lower power levels. It uses complicated switching tables.
Repetitive control	This controller is implemented as harmonic compensator and voltage controller. It shows robust performance for periodic disturbances and ensures a zero steady-state error at all the harmonic frequencies.	Is not easy to stabilize for all unknown load disturbances and cannot obtain a very fast response for fluctuating load. Can cause a slow dynamic response.
Predictive control	Possibility to include nonlinearities of the system. Allows achieving more precise voltage control with minimum THD and harmonic noise.	It is complicated and needs a lot of calculation.
Sliding mode control	Shows reliable performance during transient. Provides an acceptable THD if it is designed well.	The problem of the chattering phenomenon in discrete implementation.
PR control	Control of selective harmonics. Relatively simple structure. Ensures zero steady-state error in the stationary frame.	Sensitivity to frequency variation. Sensitivity to phase shift of voltage and current sensors.
PI control	Simple control structure. Ensures zero steady-state error in the dqo frame.	When the operating conditions change, the performance degrades. For unbalanced systems, it dos no ensure perfect performance. They are not good solution to compensate higher harmonics.
State feedback control	Good transient and steady-state performance when the system parameters are known exactly.	Extracting the model is quite complicated

four-wire microgrids is not as well established as three-phase three-wire microgrids. It may be beneficial to take an overall four-wire microgrid system, including the primary, secondary and tertiary levels when designing a control scheme.

- Considerably more work is needed to be done to exploit new control strategies for four-leg VSIs. To achieve better performance, it is necessary to use some innovative approaches such as LQR and robust control.
- Most studies neglect coupling among phases when controlling a four-leg VSI using the classical PI controller, thereby reducing the system robustness. Hence, it may be advantages to use decoupled phase voltage control to achieve precise response in time domain.

5. Conclusion

The Four-leg VSI is fast becoming a key instrument in four-wire microgrids due to its superior performance characteristics in handling unbalanced and nonlinear load conditions. An overview of different control strategies for three-phase four-leg VSIs in autonomous microgrids is presented in this paper. Furthermore, detailed analysis, comparison, and discussion on these existing control strategies are investigated. Finally, some suggestions for future research are put forward. This paper is expected to be a useful reference for researchers, engineers and manufacturers involved in four-leg VSIs.

References

[1] Basak P, Chowdhury S, Dey H, Chowdhury P. A literature review on integration of distributed energy resources in the perspective of control, protection and stability of microgrid. Renew Sustain Energy Rev 2012;16(8):5545–56.
[2] Olivares DE, Mehrizi-Sani A, Etemadi AH, Canizares CA, Iravani R, Kazerani M, Hajimiragha AH, Gomis-Bellmunt O, Saeedifard M, Palma-Behnke R, Jimenez-Estevez GA, Hatziargyriou ND. Trends in microgrid control. IEEE Trans Smart Grid 2014;5(4):1905–19.
[3] Zamora R, Srivastava AK. Controls for microgrids with storage: review, challenges, and research needs. Renew Sustain Energy Rev 2010;14:2009–18.
[4] Palizban O, Kauhaniemi K. Hierarchical control structure in microgrids with distributed generation: Island and grid-connected mode. Renew Sustain Energy Rev 2015;44:797–813.
[5] Vandoorn T, Kooning JDM, Meersman B, Vandevelde P. Review of primary control strategies for islanded microgrids with power-electronic interfaces. Renew Sustain Energy Rev 2013;19:613–28.
[6] Mirsaeidi S, Mat Said D, Mustafa W, Habibuddin M, Miveh MR. A comprehensive overview of different protection schemes in micro-grids. Int J Emerg Electr Power Syst 2013;14(4):327–32.
[7] Abdilahi AM, Yatim AHM, Mustafa MW, Khalaf OT, Shumran AF, Nor FM. Feasibility study of renewable energy-based microgrid system in Somaliland's urban centers. Renew Sustain Energy Rev 2014;40:1048–59.
[8] Miveh MR, Rahmat MF, Mustafa MW. A new per-phase control scheme for three-phase four-leg grid-connected inverters. Electron. World 2014;120(1939):30–6.
[9] Soshinskaya M, Crijns-Graus WH, Guerrero JM, Vasquez JC. Microgrids: experiences, barriers and success factors. Renew Sustain Energy Rev 2014;40:659–72.
[10] Palizban O, Kauhaniemi K, Guerrero JM. Microgrids in active network management—Part I: Hierarchical control, energy storage, virtual power plants, and market participation. Renew Sustain Energy Rev 2014;36:428–39.
[11] Rivera M, Yaramasu V, Llor A, Rodriguez J, Wu B, Fadel M. Digital predictive current control of a three-phase four-leg inverter. Ind Electron IEEE Trans 2013;60(11):4903–12.
[12] Naidu S, Fernandes D. Dynamic voltage restorer based on a four-leg voltage source converter. IET Gen Transm Distrib 2009;3(5):437–47.
[13] George V, Mishra M. User-defined constant switching frequency current control strategy for a four-leg inverter. IET Power Electron 2009;2(4):335–45.
[14] Oliveira da Silva S, Modesto R, Goedtel A, Nascimento C. Compensation algorithms applied to power quality conditioners in three-phase four-wire systems. In: Proceedings of the IEEE ISIE conference, Bari, Italy; Jul. 2010. pp. 730–735.
[15] Rocabert J, Luna A, Blaabjerg F, Rodriguez P. Control of power converters in AC microgrids. Power Electron IEEE Trans 2012;27(11):4734–49.
[16] Palizban O, Kauhaniemi K, Guerrero JM. Microgrids in active network management – Part II: System operation, power quality and protection. Renew Sustain Energy Rev 2014;36:440–51.
[17] Monfared M, Golestan S. Control strategies for single-phase grid integration of small-scale renewable energy sources: a review. Renew Sustain Energy Rev 2012;16(7):4982–93.
[18] Hassaine L, OLias E, Quintero J, Salas V. Overview of power inverter topologies and control structures for grid connected photovoltaic systems. Renew Sustain Energy Rev 2014;30:796–807.
[19] Zeng Z, Yang H, Zhao R, Cheng C. Topologies and control strategies of multi-functional grid-connected inverters for power quality enhancement: a comprehensive review. Renew Sustain Energy Rev. 2013;24:223–70.
[20] Timbus A, Liserre M, Teodorescu R, Rodriguez P, Blaabjerg F. Evaluation of current controllers for distributed power generation systems. Power Electron IEEE Trans 2009;24(3):654–64.
[21] Blaabjerg F, Teodorescu R, Liserre M, Timbus AV. Overview of control and grid synchronization for distributed power generation systems. Ind Electron IEEE Trans 2006;53(5):1398–409.
[22] Llaria A, Curea O, Jiménez J, Camblong H. Survey on microgrids: unplanned islanding and related inverter control techniques. Renew Energy 2011;36(8):2052–61.
[23] Planas E, Gil-de-Muro A, Andreu J, Kortabarria I, de Alegría IM. General aspects, hierarchical controls and droop methods in microgrids: a review. Renew Sustain Energy Rev 2013;17:147–59.
[24] Zhong Q-C, Liang J, Weiss G, Feng Chunmei, Green TC. H^{∞} control of the neutral point in four-wire three-phase DC–AC converters. Ind Electron IEEE Trans 2006;53(5):1594–602.
[25] Zhang R, Boroyevich D, Prasad VH, Mao H, Lee FC, Dubovsky S. A three-phase inverter with a neutral leg with space vector modulation. In: Applied power electronics conference and exposition, APEC'97 conference proceedings; 1997.

[26] Savaghebi M, Vasquez JC, Jalilian A, Guerrero JM. Secondary control for compensation of voltage harmonics and unbalance in microgrids. In: Proceedings of the 3rd IEEE international symposium on power electronics distributed generation systems (PEDG); June 2012. p. 46–53.
[27] Savaghebi M, Jalilian A, Vasquez JC, Guerrero JM. Secondary control for voltage quality enhancement in microgrids. Smart Grid IEEE Trans 2012;3(4):1893–902.
[28] M. Hamzeh H. Karimi H. Mokhtari J. Mahseredjian. Control of a microgrid with unbalanced loads using virtual negative-sequence impedance loop. In: Power electronics drive system and technology conference (PEDSTC); 2014. p. 78–83.
[29] Mishra M, Joshi A, Ghosh A. Control schemes for equalization of capacitor voltages in neutral clamped shunt compensator. IEEE Trans Power Deliv 2003;18(2):538–44.
[30] Meersman B, Renders B, Degroote L, Vandoorn T, De Kooning J, Vandevelde L. Overview of three-phase inverter topologies for distributed generation purposes. In: Proceedings of the 2nd international conference on innovation for sustainable production; 2010, April. pp. 18–21.
[31] Cortes P, Ortiz G, Yuz J, Rodriguez J, Vazquez S, Franquelo L. Model predictive control of an inverter with output LC filter for UPS applications. IEEE Trans Ind Electron 2009;56(6):1875–83.
[32] Liang J, Green T, Feng C, Weiss G. Increasing voltage utilization in split-link, four-wire inverters. IEEE Trans Power Electron 2009;24(6):1562–9.
[33] Zhang R, Prasad H, Boroyevich D, Lee FC. Lee. Three-dimensional space vector modulation for four-leg voltage-source converters. IEEE Trans Power Electron 2002;17(3):314–26.
[34] Lohia P, Mishra M, Karthikeyan K, Vasudevan K. A minimally switched control algorithm for three-phase four-leg VSI topology to compensate unbalanced and nonlinear load. IEEE Trans Power Electron 2008;23(4):1935–44.
[35] Savaghebi M, Hashempour M, Guerrero JM. Hierarchical coordinated control of distributed generators and active power filters to enhance power quality of microgrids. In: Proceedings of the 55th International scientific conference on power and electrical engineering of riga technical university (RTUCON); 2014. p. 259–64.
[36] Guerrero JM, Chandorkar M, Lee TL, Loh PC. Advanced control architectures for intelligent microgrids, Part I: decentralized and hierarchical control. IEEE Trans Ind Electron 2013;60(4):1254–62.
[37] IEEE recommended practice for electric power distribution for industrial plants, ANSI/IEEE Std. 141; 1993.
[38] IEEE recommended practice for monitoring electric power quality, IEEE Std. 1159; 2009.
[39] IEEE recommended practices and requirements for harmonic control in electrical power system, IEEE Std. 519; 1992.
[40] Demirkutlu E, Hava AM. A scalar resonant-filter-bank-based output-voltage control method and a scalar minimum-switching-loss discontinuous PWM method for the four-leg-inverter-based three-phase four-wire power supply. Ind Appl IEEE Trans 2009;45(3):982–91.
[41] Demirkutlu E, Süleyman C, Ahmet M. Output voltage control of a four-leg inverter based three-phase ups by means of stationary frame resonant filter banks. IEEE-IEMDC; 2007. p. 880–5.
[42] Ho CM, Cheung VS, Chung HH. Constant-frequency hysteresis current control of grid-connected VSI without bandwidth control. Power Electron IEEE Trans 2009;24(11):2484–95.
[43] Malesani L, Mattavelli P, Tomasin P. Improved constant-frequency hysteresis current control of VSI inverters with simple feedforward bandwidth prediction. Ind Appl IEEE Trans 1997;33(5):1194–202.
[44] Zhang X, Wang J, Li C. Three-phase four-leg inverter based on voltage hysteresis control. In: Proceedings of the IEEE international conference on electrical and control engineering; 2010. p. 4482–5.
[45] Liu T, Hao X, Yang X, Zhao M, Huang Q, Huang L. A novel repetitive control scheme for three-phase grid-connected inverter with LCL filter. In: Proceedings of the 7th international power electronics and motion control conference (IPEMC), vol. 1; 2012. p. 335–9.
[46] Hara S, Yamamoto Y, Omata T, Nakano M. Repetitive control system: a new type servo system for periodic exogenous signals. Autom Control IEEE Trans 1988;33(7):659–68.
[47] Chen D, Zhang J, Qian Z. Research on fast transient and $6n \pm 1$ harmonics suppressing repetitive control scheme for three-phase grid-connected inverters. IET Power Electron 2013;6(3):601–10.
[48] Cárdenas R, Pe~na R, Clare J, Wheeler P, Zanchetta P. A repetitive control system for four-leg matrix converters feeding non-linear loads. Electric Power Syst Res 2013;104:18–27.
[49] Tomizuka M, Tsao T, Chew K. Analysis and synthesis of discrete-time repetitive controllers. J Dyn Syst Meas Control 1989;111:353–8.
[50] Majid Hosseinpour, Mustafa Mohammadian, Varjani AY. Design and analysis of the droop- controlled parallel four-leg inverters to share unbalanced and nonlinear loads. Prz Elektrotech 2014:105–10.
[51] De D, Ramanarayanan V. Decentralized parallel operation of inverters sharing unbalanced and nonlinear loads. Power Electron IEEE Trans 2010;25(12):3015–25.
[52] Rodriguez J, Wu B, Rivera M, Rojas C, Yaramasu V, Wilson A. Predictive current control of three-phase two-level four-leg inverter. In: Proceedings of the International EPE/PEMC, Ohrid, Macedonia; Sep. 2010. p. T3-106–T3-110.
[53] Yaramasu V, Rodriguez J, Wu B, Rivera M, Wilson A, Rojas C. A simple and effective solution for superior performance in two-level four-leg voltage source inverters: Predictive voltage control. Bari, Italy: Proc. IEEE ISIE; 2010. p. 3127–32 Jul.
[54] Yaramasu V, Wu B, Rivera M, Rodriguez J, Wilson A. Cost-function based predictive voltage control of two-level four-leg inverters using two step prediction horizon for standalone power systems. In: Proc. IEEE APEC, Orlando, FL, USA; Feb 2012. p. 128–35.
[55] Yaramasu V, Wu B, Rivera M, Rodriguez J. Enhanced model predictive voltage control of four-leg inverters with switching frequency reduction for standalone power systems. In: Proc. EPE/PEMC Novi Sad, Serbia; Sep. 2012. p. DS2c.6-1–DS2c.6-DS25.
[56] Rivera M, Rodriguez J, Yaramasu V, Wu B. Predictive load voltage and capacitor balancing control for a four-leg NPC inverter. In: Proc. EPE/PEMC Novi Sad, Serbia; Sep. 2012. p. DS3c.8-1–DS3c.8-DS35.
[57] Yaramasu V, Rivera M, Narimani M, Wu B, Rodriguez J. Model predictive approach for a simple and effective load voltage control of four-leg inverter with an output LC filter; 2014.
[58] Yaramasu V, Rivera M, Narimani M, Wu B, Rodriguez J. High performance operation for a four-leg NPC inverter with two-sample-ahead predictive control strategy. Electric Power Syst Res 2015;123:31–9.
[59] Umamaheswari MG, Uma G, Vijayalakshmi KM. Analysis and design of reduced-order sliding-mode controller for three-phase power factor correction using Cuk rectifiers. IET Power Electron 2013;6(5):935–45.
[60] Matas J, de Vicuna LG, Miret J, Guerrero JM, Castilla M. Feedback linearization of a single-phase active power filter via sliding mode control. IEEE Trans Power Electron 2008;23(1):116–25 Jan.
[61] Yang LY, Liu JH, Wang CL, Du GF. Sliding mode control of three-phase four-leg inverters via state feedback. J Power Electron 2014;14(5):1028–37.
[62] Li Y, Vilathgamuwa DM, Loh PC. Microgrid power quality enhancement using a three-phase four-wire grid-interfacing compensator. Ind Appl IEEE Trans 2005;41(6):1707–19.
[63] Li YW, Vilathgamuwa DM, Loh PC. A grid-interfacing power quality compensator for three-phase three-wire microgrid applications. Power Electron IEEE Trans 2006;21(4):1021–31.
[64] Monfared M, Golestan S, Guerrero JM. Analysis, design, and experimental verification of a synchronous reference frame voltage control for single-phase inverters. Ind Electron IEEE Trans 2014;61(1):258–69.
[65] Rokrok E, Hamedani ME. Comprehensive Control Scheme for an Inverter-based Distributed Generation Unit. Iran J Sci Technol Trans B: Eng 2009;33(B6):477–90.
[66] Nazifi, H, Radan A. Current control assisted and non-ideal proportional-resonant voltage controller for four-leg three-phase inverters with time-variant loads. In: Proceedings of the 4th IEEE power electronics, drive systems and technologies conference (PEDSTC); 2013. p. 355–60.
[67] Wang F, Duarte JL, Hendrix MA. Grid-interfacing converter systems with enhanced voltage quality for microgrid application—concept and implementation. Power Electron IEEE Trans 2011;26(12):3501–13.
[68] Shen G, Xu D, Cao L, Zhu X. An improved control strategy for grid-connected voltage source inverters with an LCL filter. Power Electron IEEE Trans 2008;23(4):1899–906.
[69] Lei H, Fei L, Xiong J, Lin X, Kang Y. Research on paralleled three-phase four-leg voltage source inverters based on dual-loop control in $\alpha\beta o$ coordinate. In: Proceedings of the IEEE 8th international conference on power electronics and ECCE Asia (ICPE & ECCE); 2011, May. p. 2912–9.
[70] Gannett RA, Sozio JC, Boroyevich D. Application of synchronous and stationary frame controllers for unbalanced and non-linear load compensation in 4-Leg inverters. IEEE conference; 2002. p. 1038–43.
[71] Yi HZ, Jin S. Study on Control Strategy for Three-phase Four-Leg Inverter Power Supply. In: Proceedings of the 30th annual conference of the IEEE industrial eleclronics society; November 2–6 2004. p. 805–9.
[72] Vechiu I, Camblong H, Tapia G, Dakyo B, Curea O. Control of four leg inverter for hybrid power system applications with unbalanced load. Energy Convers Manag 2007;48:2119–28.
[73] Vechiu I, Curea O, Camblong H. Transient operation of a four-leg inverter for autonomous applications with unbalanced load. Power Electron IEEE Trans 2010;25(2):399–407.
[74] Cárdenas R, Peña P, Wheeler P, Clare J, Juri C. Control of a matrix converter for the operation of autonomous systems. Renew Energy 2012;43:343–53.
[75] Sinsukthavorn W, Ortjohann E, Mohd A, Hamsic N, Moton D. Control strategy for three-/four-wire-inverter-based distributed generation. Ind Electron IEEE Trans 2012;59(10):3890–9.
[76] Liu C, Wang F, Bai H. High performance controller design with PD feedback inner loop for three-phase four-leg inverter. IEEE ICIEA; 2009. p. 1057–61.
[77] B. Haoran W. Fengxiang W. Dapeng L. ChangLiang W. Tianyu A pole assignment of state feedback based on system matrix for three-phase four-leg inverter of high speed PM generator driven by micro-turbine Ind. Electron. and Appl. 1361 1366 2009 25 27.ICIEA 2009 4th IEEE Conference on May.
[78] Nasiri R, Radan A. Adaptive pole-placement control of 4-leg voltage-source inverters for standalone photovoltaic systems. Renew Energy 2011;36:2032–42.

[79] Ninad NA, Lopes L. Per-phase vector control strategy for a four-leg voltage source inverter operating with highly unbalanced loads in stand-alone hybrid systems. Electron Power Energy Syst 2014;55:449–59.
[80] Ninad NA, Lopes LAC. Unbalanced operation of per-phase vector controlled four-leg grid forming inverter for stand-alone hybrid systems. In: Proceedings of the IECON 2012-38th annual conference on IEEE industrial electronics society; October 2012. pp. 3500–05.
[81] Patel DC, Sawant RR, Chandorkar MC. Three-dimensional flux vector modulation of four-leg sine-wave output inverters. IEEE Trans Ind Electron 2010;57(4):1261–9.
[82] Zhang F, Yan Y. Selective harmonic elimination PWM control scheme on a three-phase four-leg voltage source inverter. IEEE Trans Power Electron 2009;24(7):1682–9.